Palacký University Olomouc

Faculty of Science

Department of Geology

Porosity and pore pressure Estimation from Well Log Data of Tertiary Khurmala Formation, Kurdistan Region/Iraq

Bachelor thesis

Aran Hamashareef

Petroleum Engineering (B0724A330002)

Fulltime study

Supervisor: Prof. Mgr. Ondrej Babek

Olomouc 2023

Anotace:

Terciérní khurmalské souvrství je lagunový krystalický vápenec, dolomit s vložkami různých klastických hornin. V některých záhonech se také vyskytuje občasný výskyt sádrovce a vzácných plžů, miliolidů a řas. Útvar tvořil dolostone a dolomitický vápenec s vsunutými jílovitými vrstvami mezi zjištěnými vrstvami. které lze považovat za dobrou nádrž z hlediska pórovitosti, zatímco obsah břidlice snižoval kvalitu nádrží těchto jednotek. Útvar má proměnlivou mocnost v celém poli, 99,8 m od severovýchodního okraje a 109 m v jihovýchodním ponoru a v jiné oblasti má různou mocnost. Pórový tlak a kompartmentalizace rezervoárů budou studovány za účelem řízení změn tlaku v karbonátových rezervoárech během průzkumu ropy. Metodu Eaton lze použít k predikci tlaku v pórech z dat zvukového záznamu. Základním předpokladem je vzájemný vztah mezi pozorovanou dobou průchodu z log čtení a normální dobou průchodu, která se nachází na trendu normálního zhutňování (NCT). Objemovou hustotu lze určit ze zvukového logaritmu a ukázat shodu s objemovou hustotou odvozenou z logaritmu hustoty, aby se prokázalo, že zvukový logaritmus lze použít jako dobrou alternativu k získání sypné hmotnosti a následně ke stanovení litostatického tlaku. Pórový tlak závisí na změnách gradientu nadloží a obsahu tekutiny. Na základě předpokládaného tlaku v pórech lze prostor studovaného zásobníku rozdělit na tlakové zóny. Gama-ray log, hustota a neutron log se používají k odhadu pórovitosti a litologické identifikaci. Popisy vzorků hornin a mikroskopické studie tenkých řezů lze také použít ke vzájemnému ověření a ověření pórů z log dat. Studie závisí na práci v terénu, mikroskopických studiích, laboratorním měření pórovitosti a propustnosti a analýze jamek. Metody studia jsou (Digitalizace těžebních dat, Identifikace trendů normálního zhutňování, Stanovení tlaku v nadloží a pórového tlaku, Zhotovování a studium tenkých řezů a Měření pórovitosti a propustnosti vzorků hornin). Záznam gama záření odhalil, že objem břidlice v khurmalském souvrství je 20 %, a křížový graf neutronové hustoty ukázal, že nádrž se skládá převážně z vápence a dolomitického vápence. Model pórovitosti ukázal, že ve spodní části raně třetihorní formace je přítomna dobrá a dobrá pórovitost a propustnost, a model nasycení ukázal, že horní část formace nemá žádný důkaz uhlovodíku, ale jsou přítomny dobře pohyblivé uhlovodíky. Predikce a modelování pórového tlaku na základě sonického logaritmu ukázaly, že k pórovému tlaku ve formaci dochází po hloubce 1550 m a normální trend zhutňování se zvyšuje směrem k větší hloubce formace.

Anotation:

The Tertiary Khurmala Formation is a lagoonal crystallized limestone, dolomite with interbeds of different clastic rocks. It also contains an occasional occurrence of gypsum and rare gastropods, miliolids, and algae in some beds. The formation comprised dolostone and dolomitic limestone with intercalation of clay layers between the recognized beds. that can be considered as a good reservoir unit in terms of porosity, whereas the shale contents reduced the reservoir quality of these units. The formation has variable thickness throughout the field, 99.8 m from the northeastern limb and 109 m in the southeastern plunge and it has a different thickness in another area. Pore pressure and reservoir compartmentalization will be studied to manage pressure changes in carbonate reservoirs during petroleum exploration. The Eaton method can be used to predict the pore pressure from sonic log data. The basic assumption is the interrelation between observed transit time from log reading and normal transit time that locates on the normal compaction trend (NCT). The bulk density can be determined from the sonic log and show matching with the bulk density derived from the density log to demonstrate that the sonic log can be used as a good alternative to obtain the bulk density and consequently to determine lithostatic pressure. Pore pressure depends upon changes in the overburden gradient and fluid content. Based on predicted pore pressure, the study reservoir compartment can be divided into pressure zones. Gamma-ray log, density and neutron log are used to estimate porosity and lithology identification. Rock sample descriptions and microscopic study of thin sections can also be used to validate each other and pores from log data. The study depends on the fieldwork, microscopic studies, lab measuring porosity and permeability, and well log analysis. Study methods are (Digitizing of well log data , Identification of normal compaction trend, Determination of overburden pressure and pore pressure, Making and studying thin sections, Measuring porosity and permeability of rock samples). The gamma ray log revealed that the volume of shale in the Khurmala Formation is 20%, and the neutron-density cross-plot showed that the reservoir consists mainly of limestone and dolomitic limestone. The porosity model showed that fair and good porosity and permeability are present in the lower part of the Early Tertiary formation, and the saturation model showed that the upper part of the formation has no evidence of hydrocarbon but good movable hydrocarbons are present. Pore pressure prediction and modeling based on sonic well-log showed that the formation pore pressure

occur after depth 1550m, and normal compaction trend has increase toward the more depth in the formation.

Klíčová slova: Pórovitost, Pórový tlak, Studna, Formace Khurmala

Keywords: Porosity, Pore Pressure, Well log, Khurmala Formation

Number of pages: 49

I declare that I have prepared the bachelor's thesis myself and that I have stated all the used information resources in the thesis.

In Olomouc, February 27, 2023 ……

Aran Salar Hamashareef

Acknowledgement

Acknowledgements First and foremost, I offer my sincere gratitude to my supervisor Prof. Mgr. Ondrej Babek and also my Adviser mr Hussein.Hussien, for their willingness to supervise my research. their endless support, direction and encouragement have helped me a lot during the writing up of my study. I would like to thank my dearest parents for their undying love, patience and support, Without their encouragement, it would have been impossible for me to continue and finish my studies. I would like to show my appreciation to all my teachers and classmates at Palacky University, particularly in Petroleum Engineering and Geology Department for their support I get it during the writing up of my research.

Table of Contents

List of Figures

Chapter 1:Introduction

1.1 Preface

The Kirkuk Group, Euphrates Formation, and Jeribe Formation have been identified as the three main reservoir rocks in the Tertiary petroleum system in the Zagros folded zone, Kurdistan region, Iraq, according to Jassim and Goff (2006). The Eocene Avanah Formation and Paleocene Sinjar Formation, which comprise the Avanah and Khurmala domes, are among the main reservoir rocks of the Kirkuk oil field (Aqrawi et al., 2010). Additionally, the Chamchamal block, Taq Taq, and Tawke oil fields in Kurdistan's Zagros basin have anisotropic reservoir rock units from the Eocene Pilaspi Formation.

On the other hand, neither newly discovered fields in the Kurdistan region nor previously established fields in the Tawke oilfields have shown the Paleocene Khurmala Formation as a producing reservoir rock. Therefore, in order to understand the reservoir potentiality of this deposit, only a very limited amount of study on the reservoir characterization of this interval in the tertiary petroleum system was addressed. The Khurmala Formation's petrophysical properties and reservoir quality were assessed in this study using subsurface data sets from the Tawke oil field in order to identify the logical factors that affected the rock's capacity to retain hydrocarbons and production efficiency.

The Khurmala Formation in northern Iraq has been studied for a long time. Bellen, 1953 recognized the Khurmala Formation for the first time in well K-114 at Kirkuk. The formation contains oolitic dolomite and crystalline limestone that interfinger with sandstone beds (from the previous Kolosh Formation) that contain clasts of chert, flint, radiolarite, and greenstones of silt and sand size. Anhydrite (perhaps secondary) is also occasionally found (Bellen et al., 1959).

1.2 Geological setting

In the Late Cretaceous to Early Miocene, the Arabian and Eurasian plates collided, creating the Zagros Mountains. The Iranian Plateau and the Zagros Mountains both gain height annually as a result of this process, which is still active today at a rate of around 25 mm year-1. In the southeast of Iran, the Zagros Mountains are a strip of deformed crustal rocks. From eastern Turkey in the northwest through the Gulf of Oman in the southeast, they span a distance of more than 1500 kilometres. From northeast to southwest, Alavi (2004) classified the Zagros orogen into three tectonic units: the Urumieh-Dokhtar magmatic assemblage, the Sanandaj-Sirjan zone (the Zagros imbricate zone), and the Zagros Fold-Thrust belt (Fig.1). This belt's deformation intensity increases towards the northeast (Alavi 1994). The Stable Shelf, the Unstable Shelf, and the Suture Zone are the three principal tectonic zones that Jassim and Goff (2006) identified in Iraq's Zagros orogenic belt. Mesozoic and Cenozoic periods yield short-wavelength, high amplitude folds with south to southwest vergences in the high folded zone (Fouad, 2014). The deformation style of fault-related folds is halfway between fault-bend folds and fault propagation folds (Zebari, 2013). As one proceeds north and northeast, the amount of shortening and the intensity of deformation increase (Fouad 2014). In the northern region of Iraqi territory, the Zagros-Taurus Fold and Thrust belt contains the Tawke anticlinal structure. This structure is situated in the tectonic transition zone between the Low Folded Zone to the south and the Imbricated Zone to the north in Iraq. It was clear that the area's topography was reflecting structural elements. Folds, faults, and large cracks have a crucial role in forming or adding complexity to the region.

The Tawke Oil field is located within the Tawke anticlinal structure in the city of Zakho-Duhok governorate, northern Iraq, and is elevated 500 m above sea level. The Tawke oil field is located in the Zagros-Taurus Folds and Thrust belt's High Folded Zone. It is one of Iraq's greatest oil fields, producing high-gravity oil from a fractured reservoir at a depth of less than one kilometer. DNO, the Norwegian oil and Gas Company, redeveloped the field beginning in 2004 and began production in June 2007. Early in 2009, the Tawke export infrastructure was linked to the Iraq-Turkey pipeline system to provide crude oil to the international market (Mzuri and Omar, 2016).

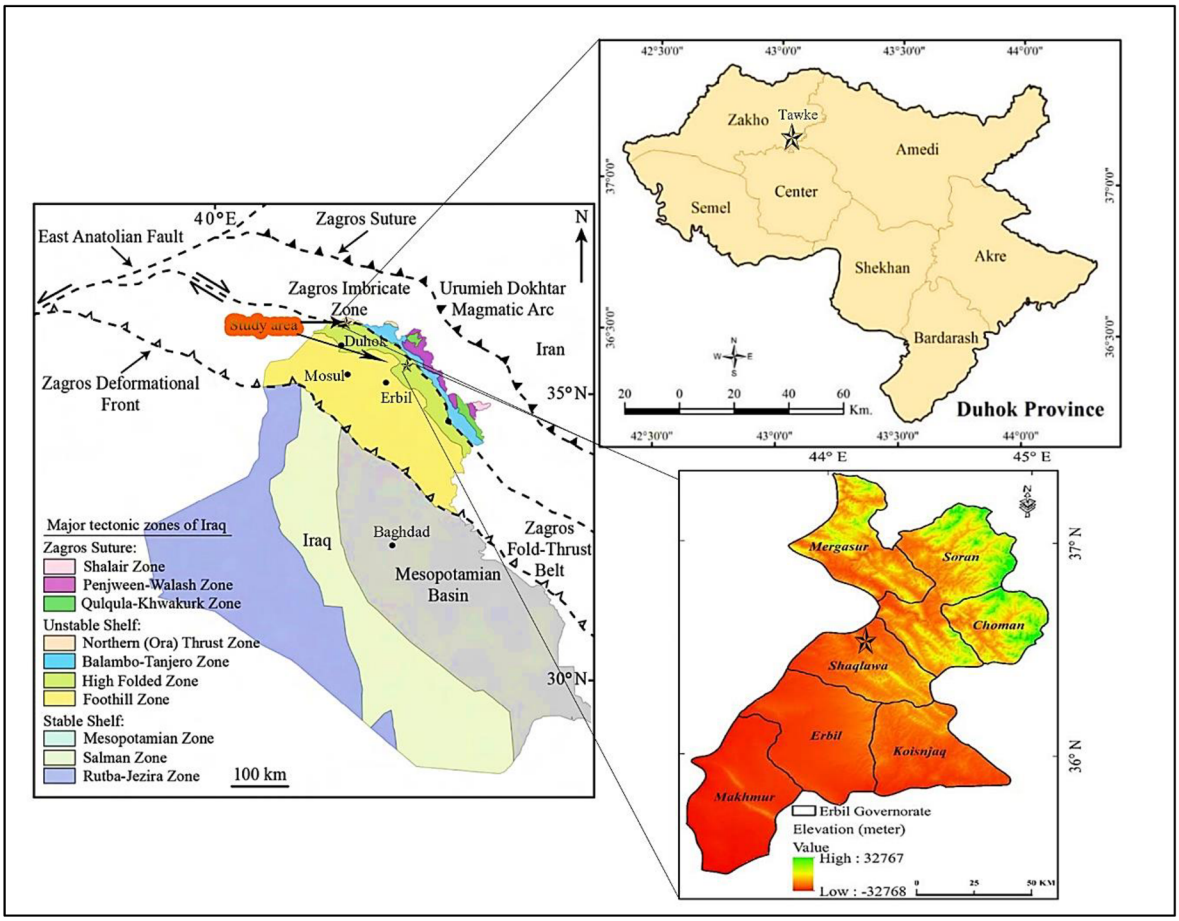

Figure 1 Tectonic map of Iraq showing the studied area (Doski 2019)

1.3Aims of the study

The main objectives of this study are:

1-Petrographic study to identify microfacies and porosity of the Khurmala Formation in the studied area.

2-Determination of petrophysical properties such as porosity, shale content, water, and hydrocarbon saturation based on set of wireline log data.

3-Estimation of pore pressure and compartmentalization of the reservoir, using core sample data.

Chapter 2: literature Review

Nearly 15% of the world's hydrocarbon reserves are located in the Middle East, where carbonate rocks are the predominant producing reservoir type (Hollis, 2011; Hollis et al., 2017; Jafarian et al., 2017; Adam et al., 2018). The Zagros basin in Iraq is characterized by the extension of various petroleum systems and the heterogeneous distribution of reservoir types, including Triassic (Ryder Scott, 2011), Jurassic (Sherwani and Zangana, 2017), Cretaceous (Al-Qayim and Rashid, 2012; Rashid et al, 2017; Ghafur and Hasan, 2017) and Tertiary reservoir rocks (Al-Qayim and Othman, 2012; and Hussein et al., 2018).

The Khurmala Formation sediments are found in various locations throughout north Iraq as tongues within the upper part of the Kolosh Formation (Early Eocene age, Alveolina primaeva and Saudia labyrinthica appear to be restricted to the Late Palaeocene; Daviesina, Dictyokathina simplex, Idalina sinjarica, Miscellanea miscella, Nummulites fraasi and Operculina salsa to the Late Palaeocene-Early Eocene; and Alveolina oblonga and Assilina placentula to the Early-Mid Eocene.). The formation is 185 meters thick in the type area, 173 meters thick in Kirkuk 117, 115 meters thick in Taq Taq-l, and 262 meters thick in Atshan1. Because of the presence of sediments from the underlying series, the measured thickness in well Jabal Kand-l of 606 m is probably too high.

Al-Banna et al. (2006) studied Khurmala Formation at Bekhair anticline and showed a bundle of mixed carbonate and clastic sediments, measuring about 60 meters thick and dating to the Early Eocene, makes up the examined surface part of the Khurmala Formation, which is located northeast of Duhok city in northern Iraq. The clastic material contained two lithofacies associated with the depositional environment of estuaries, whereas the carbonate sediment is composed of four microfacies associations assigned to shoal bank (Kh2), lagoon (Kh1), intertidal (Kh1, Kh3), and supratidal (Kh4). The Khurmala Formation was given a depositional model. Microfacies exhibit diagenetic dissolution and dolomitization processes (Kh3)(fig. 2).

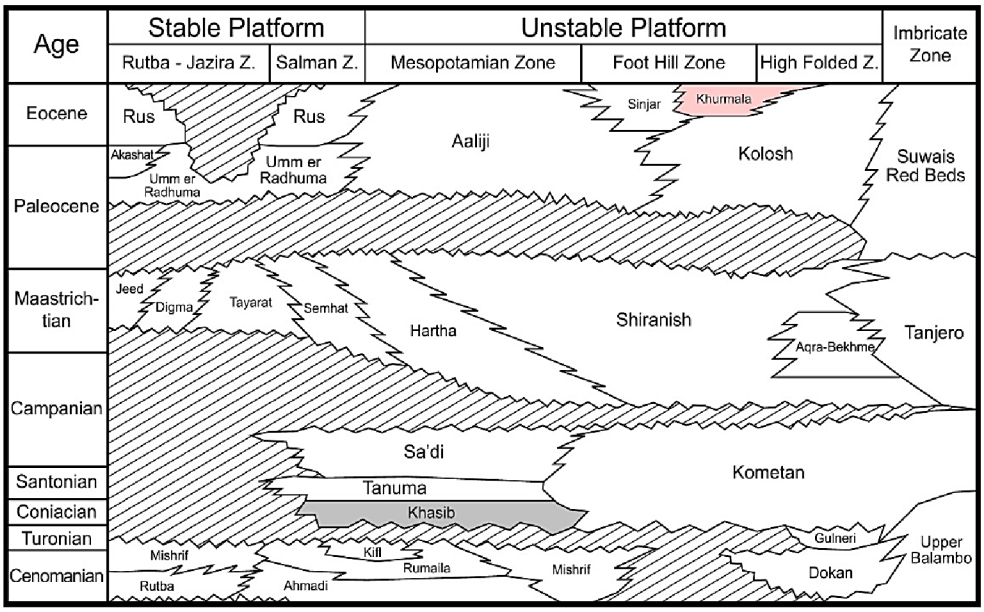

Figure 2 Chronostratigraphy chart of tertary and cretaceous sections in Iraq after Van Bellen et al., 1959, Buday, 1980, Jassim and Goff, 2006

Al-Lihaibi (2012) studied Khurmala Formation in Dokan area and he claimed within the Khurmala limestone Formation in the Dokan region of northeastern Iraq, diagenesis was investigated. The study identified a number of diagnostic mechanisms. a series of processes, including micrite envelope, dolomitization, dissolution, neomorphism, cementation, and mechanical and chemical compaction, influenced the limestone. The investigation identified four diagnostic zones. They are the burial zone (mechanical and chemical compaction), mixing zone, meteoric phreatic zone (dissolution, neomorphism, cementation), and marine zone (micrite envelope). The study found that periodic changes in sea level have had an impact on diagenetic processes and their paragenetic sequence, according to the history of diagenesis and their sequence.

Assad and Balaky (2018). In the Zenta area of the Aqra district in northern Iraq's Kurdistan region, the microfacies and environmental studies of the Khurmala Formation were studied. The formation is composed of medium to thick bedded yellow limestone that is interbedded with thin layers of marl and mudstone, as well as bedded grey dolomitic limestone that is primarily bituminous with chert nodules. Three significant microfacies, as well as two different lithological units, were found in the limestones of the investigated region based on

field evidence and petrographic study. dolomitic limestone unit with thick bedding and the marl limestone unit with bedding. Petrographic data, facies, and textural studies suggest that the shelf lagoon setting of a shallow marine environment is where the Khurmala Formation was deposited.

Rashid et al., (2020) investigated the Khurmala Formation in the Taq Taq oil field utilizing wireline log analysis, drilling cuttings, and fluid distribution to better understand reservoir potentiality and fluid dispersion. The formation was composed of dolostone and dolomitic limestone, with clay layers intercalated between the known strata. The computed shale volume shows a high rate of clay content, with some spots of the gamma ray containing 100% shale. The Authors divided classified the Khurmala Formation into five porosity units based on the corrected log-derived bulk porosity (Kh-1 to 5). The first (Kh-1), third (Kh-3), and fifth (Kh-5) porosity units had an average porosity of more than 10%, which is regarded an excellent reservoir unit in terms of porosity, however the shale component of these units affected the reservoir quality.

Al-Qayim and Barzani (2021) studied facies and stratigrapy of Khurmala Formation in Duhok Area and based on field observations, along with microscopic investigations, they identified facies types of the formation. The Khurmala Formation in Spindar and Birkyat seems to be deposited in a shallow shelf setting of supratidal, intertidal, and semi-restricted lagoonal facies with siliciclastic-dominated coastal plain.

Assad et al. (2022) studied the depositional environment of the Khurmala Formation (Paleocene-Eocene) in Iraq's High Folded Zone has been examined in the Nerwa section, the southern limb of the Berat anticline. The formation consists of three units: fossiliferous bedded limestone, massive dolomitic limestone, and bedded marly dolomitic limestone. Based on petrographic study of carbonate rocks, five primary microfacies were identified: lime mudstone, lime wackestone, lime packstone, grainstone, and boundstone, as well as one lithofacies, an intraformational conglomerate. Based on microfacies and the field characteristics of the Formation, two facies associations were established that indicate deposition in a lagoonal environment including reef patches.

Chapter 3: Material and methods

3.1 Technical methods and material

The porosity and permeability were calculated using log data. The environmental adjustments and reservoir parameters like porosity, relative permeability, water, and hydrocarbon saturation (fluid content) were computed using a software tool. The digitized LAS files, which comprise caliper gamma ray, density, neutron, acoustic, and resistivity records, are loaded into the Interactive Petrophysics program (IP-V 4.4). The reading measurements are obtained as one reading per 0.2 meters. The log curves are evaluated for depth with each other. The depth-matched log curves were then compared to the available gamma ray data, which were used as a reference guide for the depth evaluation.

On the other hand, the pore pressure models allow you to evaluate the subsurface pressure encountered within a well, then enable you to model the overburden pressure, and pore pressure within the lithology. The rock physics modules can be found under advanced interpretation- rock physics.

The first step of the module is to perform a density estimation calculation based on the sonic curve within the data set. In this section develop density curves using the P-wave (Vp) velocity and imperial relationships. The lithology used is either gardener, Bellotti, or Lindseth. Here we generate an output set so the curves made can be easily identified later on. Select run to perform calculations, this will then generate the curves.

The next step is to perform an overburden gradient calculation, for overburden gradient calculations a depth curve is required, additionally, Kelly bush (KB) height or water depth and water density require to be used, now select the density curves previously made for the gardener, Bellotti or Lindseth. Next, name your output curve set as required. In this study, a new curve set has been made so the curves will be easy to identify. Select Ok to perform the calculation. As you see two new curves have been added to the well. Then press make plot to examine the results.

The final step now is to run the pore and fracture pressure gradient calculations. Input the well data. Select the previously made overburden gradient, select depth curve and the shale discriminator curve. The Kelly bushing height, water depth and water density will be automatically filled from the well header information here we must choose appropriate units

The next stage is determining what the pore pressure gradient and pressure will be calculated from, here using sonic curve. Next select the method for calculating fracture gradient and pressure, either select from Eaton, Mathew or baker or wood.

In this study, the Eaton method will be used, select the output curve again that will be computed after the analysis has run then select pore pressure tolerance percentage

In the general tab you can set the depth interval over which the analysis is performed the shale cut-off and the hydrostatic gradient and the hydrostatic gradient units.

The next stage is inputting the well data. The first sub tab is the casing string, input information leak off test pressure. And the compute mud weight.

The final tab is the results cross plot tab, choose to display the plotted model as depth vs. pressure or depth vs. pressure gradient

Final press Ok and see the results, the pore pressure is calculated in shale intervals.

The vertical line of the shale discriminator track is the shale cut-off

3.2 Thin section analysis

A thin section is a thin slice of rock only 30 microns thick which glued to a glass slide. First operation is to cut rocks by rock saw machine (Fig.3) for suitable size for polishing and gluing it to the glass (Fig.4) the next step is in thin section process is grinding and polishing the rock sample to be epoxide to the glass on the glass plate and powdered grits .Then grinding of one side of the glass and then gluing the rock samples to the glass and cutting the remaining rock after gluing the glass to the rock sample the thin section will be done and it will need grinding the thin section on the glass plate and by powdered grits (Fig.5) after a having a smooth side in the thin section it will need the polishing by a machine (Fig.6).

Measuring porosity in the thin sections measured by a program which is called (ImageJ).

Thin sections which are used in this project is taken from seven samples from Shaqlawa out crop in Kurdistan Region of Iraq (fig. 7)

Figure 3 Rock cutting machine at the Palacky University lab

Figure 4 rock sample with polished and grinded with glass plate and powder

Figure 5 thin section sample grinded with glass plate and powder

Figure 6 thin section polishing machine

3.3 Core sample process

Core plugging apparatus used to make core plugs from rock samples taken from carbonate outcrops. The plugs were ready for the core flooding experiments. This equipment allows core plugs with diameters of 1 to 1.5 in and lengths of 3.5 to 3.5 in. after this the Core cutter apparatus by altering the plug dimensions, the core cutter device was used to change the shape of the created core samples. A cutter machine is used to cut the modification surface and flatten the core surface. The cutter machine was used to produce thin sections for wettability testing in addition to cutting the core. Extraction using the Soxhlet method the pores within the core contain a variety of fluids that must be cleaned before the core flooding test can be done. before core flooding the core, plugs were cleaned with a soxhlet extraction. A heater, solvent cup, sample chamber, condenser, and cooling pump are all part of the soxhlet apparatus. The core plugs were dried in an oven after being cleaned. The oven used in this study was built by the Day Tajhis Aryan Paya (D.T.A.P) Company and can attain temperatures of up to 200 degrees Celsius. porosity meter was used to assess the porosity of the cores. This device evaluates porosity by injecting helium gas into the core sample, which is based on Boyle's and Charles' Law. A gas permeameter was used to determine the permeability of the core plug samples. The apparatus was built to measure permeability while taking into consideration the slip factor and Solution permeability at varied flowrates, back pressures, and injection pressures. A differential pressure transmitter was use to track the differential pressure on both sides of the core sample, and a precision mass flow meter was used to estimate the gas flow rate through the sample

Four samples used for porosity and permeability measuring which they are from Shaqlawa out crop in Kurdistan Region of Iraq (fig.7)

Figure 7 Shaqlawa out-crop in Kurdistan region of Iraq

Chapter 4: Determination of petrophysical properties

4.1. Lithology and mineralogy

A wireline log was used to integrate the lithological description, and a sonic-neutron log cross-plot was used to identify the lithology (Rider and Kennedy, 2011; Krygowski, 2003; Schlumberger, 1997). The most popular combination approach for determining lithology uses the overlapping and crossing between the neutron-density and neutron-sonic logs. Furthermore, a crucial conclusion for continuous lithological fluctuations in recorded intervals is provided by the cross plot between a neutron and sonic log. By using this procedure, you may obtain a single rock type or a combination of two different rock types, such as limestone, dolostone, or dolomitic limestone. Based on the mentioned cross-plot the Khurmala Formation in Tawke-1 consists mainly of limestone and dolomitic limestone (Fig.8) showed that the most plotted points are located on the limestone line where the porosity between 10-15% while the other points have high porosity located between limestone and dolomite lines or as can say dolomitic limestone

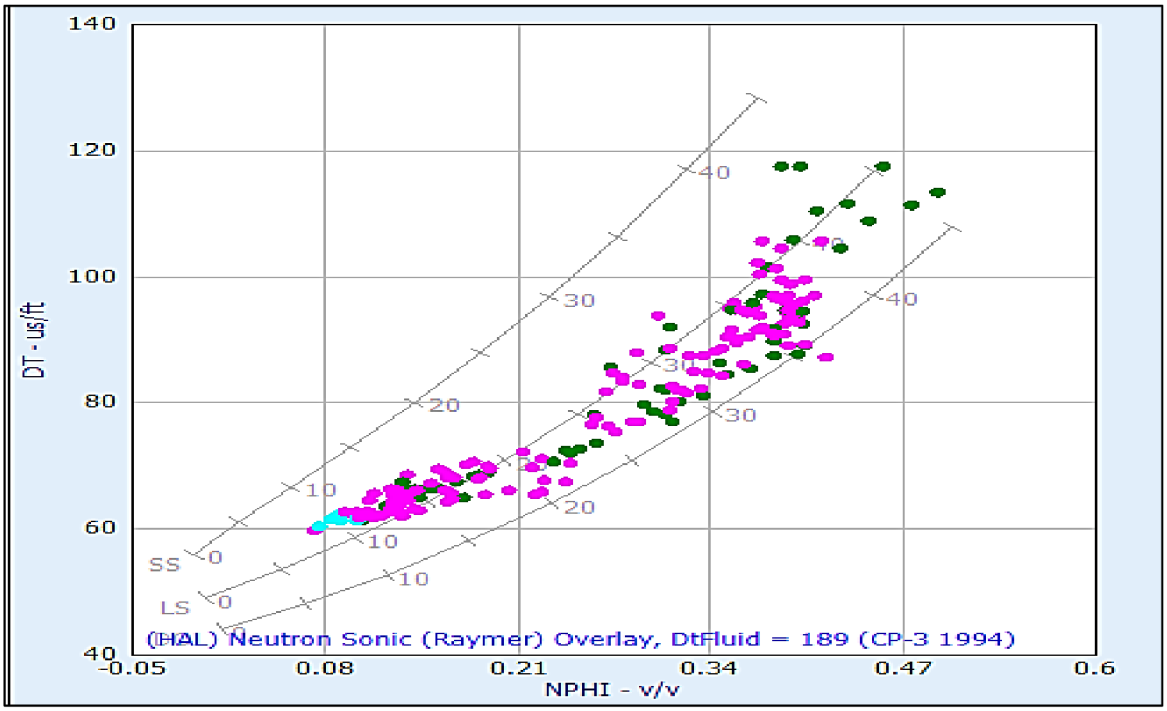

Figure 8 relationship between DT and NPHI shows the lithology of Khurmala Fm.

The M-N cross-plot may also be used to determine the formation's lithology and mineralogy. When the lithology of a formation is more complicated, this approach is applied. This cross-plot requires the acoustic log in addition to the neutron and density logs. The sonic log is a porosity log that quantifies the transit time between intervals (Asquith and Gibson, 1982). Calcite and dolomite are the primary constituents of the Khurmala Formation, according to the M-N cross-plot with some shale that has been observed (Fig. 9).

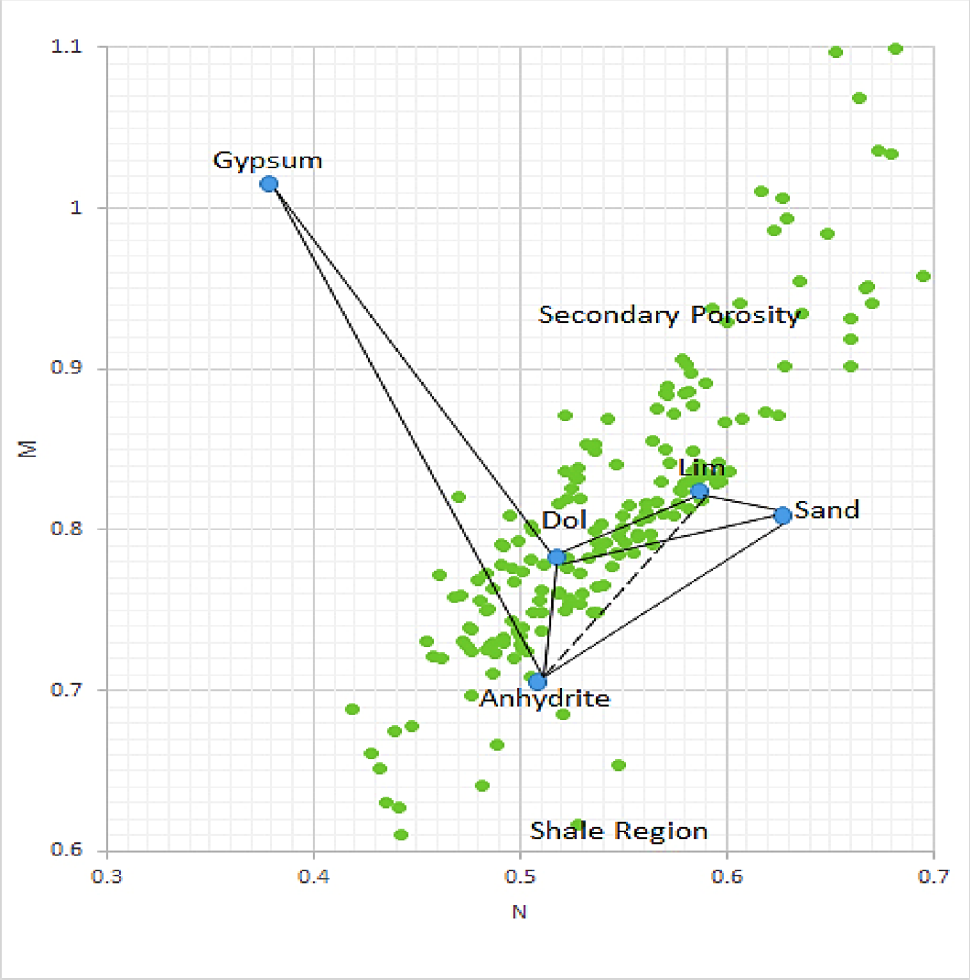

Figure 9 M-N relationship showing that the selected formation consists of limestone and dolomite with some points scattered to shale region and secondary porositzy (Asquith and Krygowski 2004)

4.2. Shale Volume

The volume of shale (clay) in a certain interval may be calculated using the gamma ray log. Shale volume is the estimated volume, which is often represented as a decimal fraction or percentage (Vsh). Because organic matter may concentrate uranium, its presence in carbonate rocks may have an impact on how much shale is present. The first step in calculating the shale volume using (Equi.1) is to calculate the gamma ray index (I_{GR}), using the shale baseline (gamma reading = 100 API), clean sand line (gamma reading = 0.0 API), and the gamma ray log measurement from the chosen interval (Bhuyan and Passey, 1994). The best equation is then used to convert the computed gamma ray index (IGR) to shale volume. The Larionov (1969) equation for estimating the amount of shale in Tertiary (young) rocks was employed in this investigation (Equi. 2).

$$\mathrm{IGR} = \frac{\mathrm{GR\,log} - \mathrm{GRmin}}{\mathrm{GR\,max} - \mathrm{GRmin}} \quad \cdots\cdots\cdots\cdots\cdots\cdots (1)$$

$$Vsh = 0.33(2^{2*GRI} - 1) \cdots\cdots\cdots\cdots\cdots (2)$$

I*GR*: Gamma ray index

GR*log*: Gamma ray reading from log, API

GR*min*: Minimum gamma ray reading (clean sand or carbonate), API

GR*max*: Maximum gamma ray reading (shale), API

V*sh*: Shale volume.

The Khurmala Formation has a maximum gamma ratio of 62 and a lowest gamma reading of 23, as seen in (fig 10). The formation has an average clay concentration of 20%, showing that the chosen formation normally includes more clay, which has an impact on reservoir attributes since a lower shale content often displays clean zone while an increase in shale volume reduces the effective reservoir capacity.

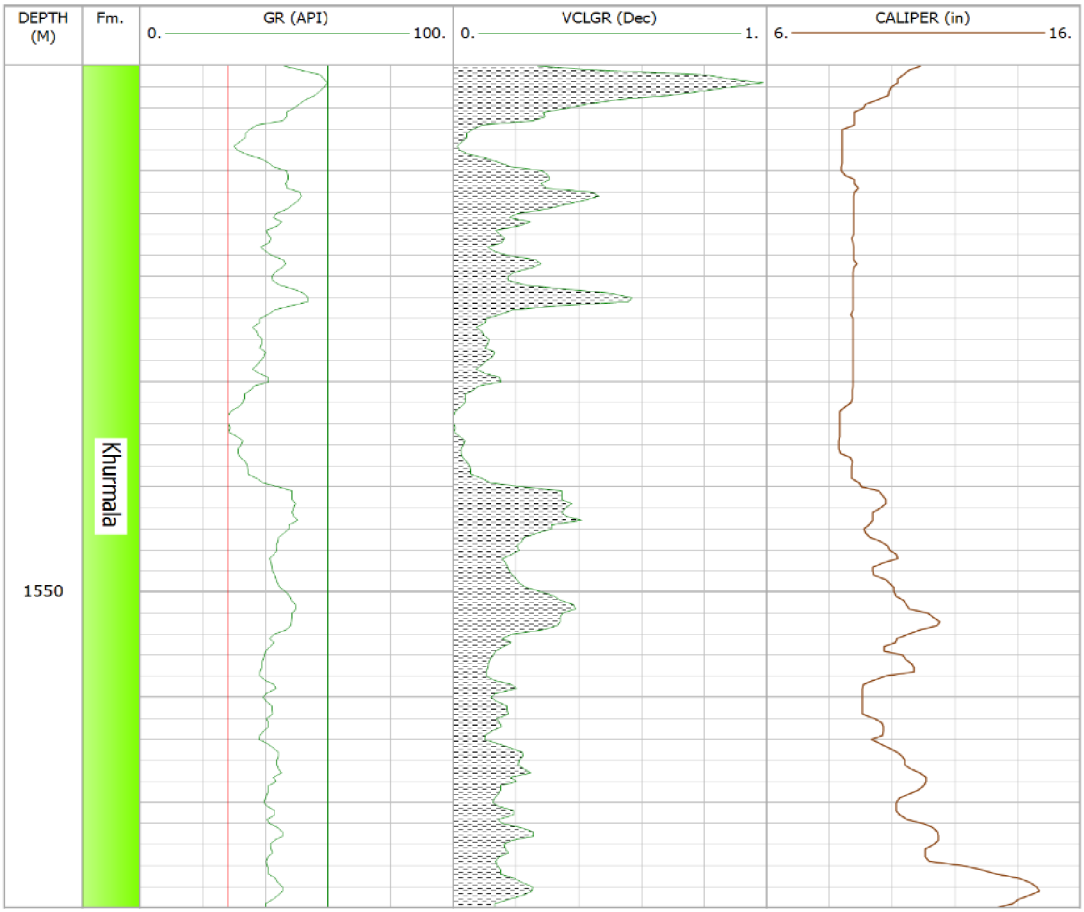

Figure 10 Calculated the Volume of shale in the Khurmala Formation from (Tawke-1) welll

4.3. Water resistivity (Rw)

The Pickett cross-plot, which is a visual representation of Archie's idea, was first presented by Pickett in 1966. By plotting the true resistivity (Rt) on the horizontal axis and the effective porosity (φe) on the vertical axis using logarithmic scales for both axes, the parallel lines that represent the water saturation (Sw) may be created. You may read the whole Sw of any plotted point. This approach is based on the idea that porosity, water saturation, and cementation factor (m) all affect real resistivity. The line at complete saturation with water represents the wet resistivity (Ro). On the real resistivity scale, when porosity equals one and the line with a slope of (-1/m) intercepts the vertical scale, water resistivity may be read. The formation water resistivity in the selected interval is too low (0.063) which indicate that the formation water saturation and watercut not reached to 20% and water free hydrocarbon can be produced in the selected formation, in addition to, this relationship has also been used to calculate the values of the a, n, and m parameters that can be seen on the (Fig.11).

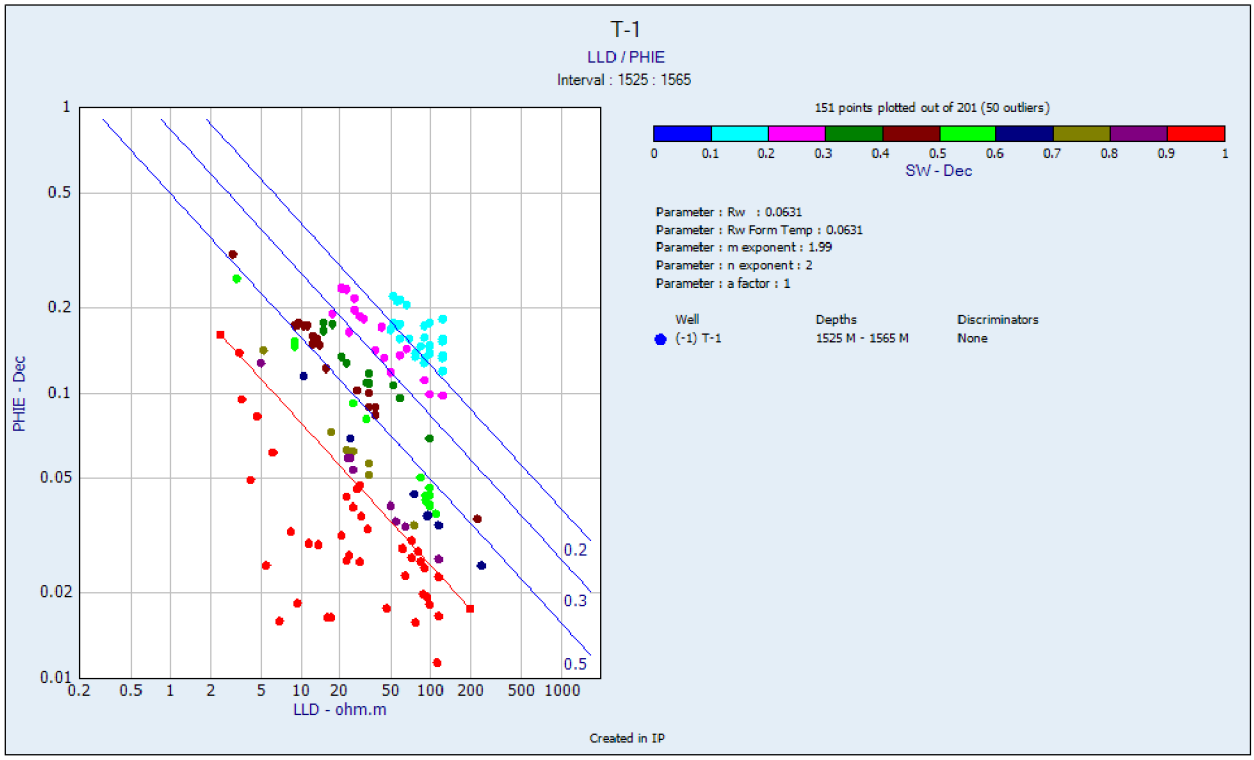

Figure 11 True resistivity vs. effective porosity showing Rw value of the Khurmala Formation in Tawke oilfield

4.4. Buckles model

A cross plot of porosity and water saturation is used to determine the bulk volume of water. Since the amount of water produced by a well may have an effect on the economy, it is essential to comprehend the total volume of water and the irreducible saturation of water (Swirr) (Asquith and Krygowski 2004). As can be seen, the Khurmala structure is equally dispersed around the hyperbolic line 0.02 and 0.04 (Fig. 12), implying that the reservoir is homogenous and irreducibly saturated with water. When the volume of bulk water follows hyperbolic lines and is nearly constant, the composition is homogenous and at irreducible water saturation.

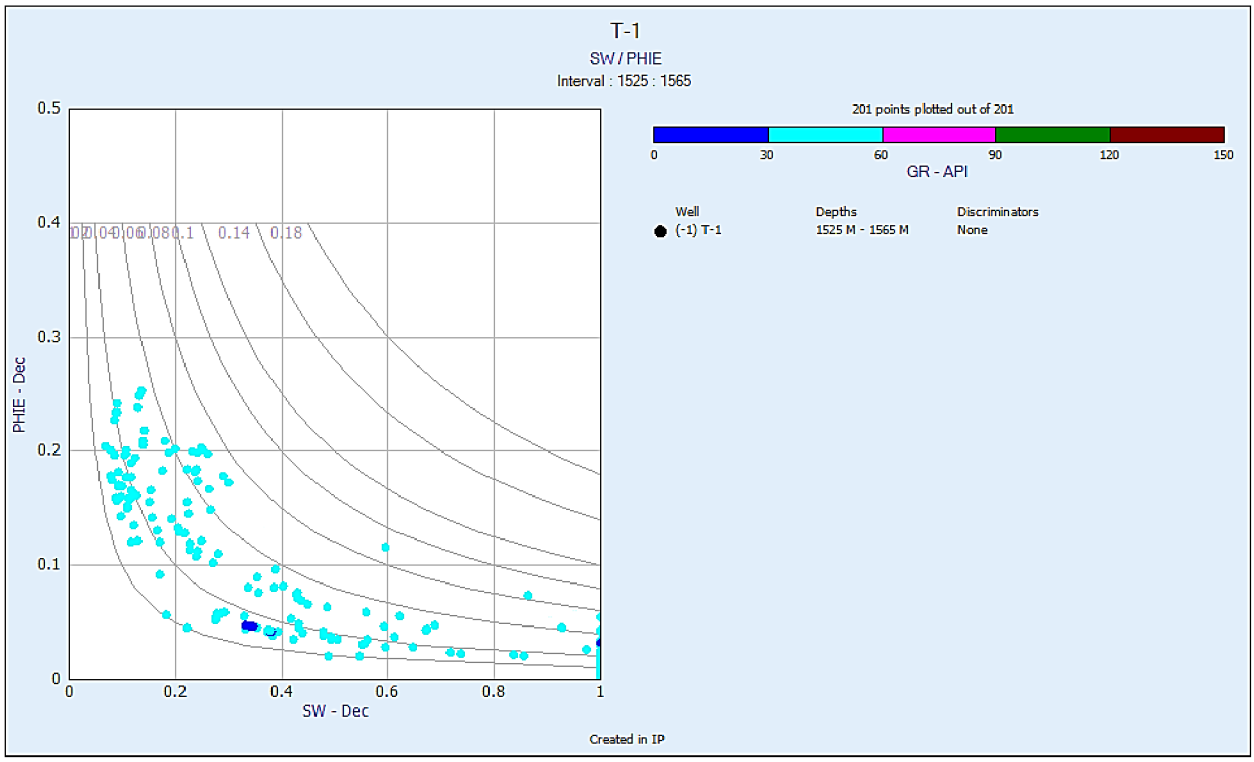

Figure 12 Buckle model showing the points of the studied formations on 0.02 hyperbolic and is at irreducible water saturation

4.5 Porosity

Porosity logs—also known as sonic, density, and neutron logs—are extensively used to measure porosity in formation evaluation and reservoir quality assessment. Wiley time average (Equi.3) (Wiley and Pachett, 1990; Asquith and Krygowski, 2004) must be used to compute porosity from the sonic slowness and the apparent density of the fluids inhabiting the pores using the matrix's values (Equi. 4). Additionally, when reading the recorded period, the hydrogen concentration was instantly

$$\boldsymbol{\Phi}\text{S} = \frac{\Delta tlog - \Delta tma}{\Delta tfl - \Delta tma} \ldots\ldots (3)$$

ϕs: Sonic porosity, fraction

$\Delta t\ log$: Sonic log reading, μs/m

$\Delta t\ ma$: Transit time of matrix, μs/m

$\Delta t\ fl$: Transit time of the mud filtrate, μs/m.

$$\Phi\ \rho\ = \frac{\rho ma - \rho b}{\rho ma - \rho f} \ldots\ldots (4)$$

$\Phi\rho$: Density porosity, fraction

ρma: Matrix density, g/cm^3

$\rho bulk$: Log reading density, g/cm^3

ρfl : Fluid density, g/cm^3.

ΦN= neutron log index

If the formation contains non-gas fluid the formula is

$$\Phi\text{t} = \Phi\text{D} + \Phi\text{N}/2 \ldots\ldots\ldots\ldots\ldots (5)$$

If the formation contains gas fluid the formula is

$$\sqrt{\frac{\Phi\text{D}2 + \Phi\text{N}2}{2}} \ldots\ldots\ldots\ldots\ldots (6)$$

Effective porosity equation

$$\text{Øe} = \text{Øt} * (1 - \text{Vsh}) \ldots\ldots\ldots\ldots (7)$$

The density and neutron tools both employ nuclear measurements, whilst the sonic tool evaluates the acoustic qualities of the rock. The combination of three porosity logs in reservoir properties measurement yields an accurate value of the computed porosity using wireline logs. The estimated porosity in this study was obtained using porosity logs adjusted for shale content.

Carbonates lose porosity owing to a combination of pressure dissolution, compaction, and cementation (Mukherjee and Kumar 2018). Because the shale proportion in the Khurmala Formation fluctuates between 19% and 20%, there is a discernible variation between effective and total porosity., The investigated period is divided into two zones (1, 2), both of which are 20m thick (Fig. 12).

4.6. Permeability (K)

4.6.1 Determine permeability from well log

Permeability is the second most important characteristic of a reservoir; the pores must be connected to allow hydrocarbons to flow in and out of the reservoir. Permeability is one of the most important variables in a reservoir since it refers to the ability of the liquid to move through the rock and is a major regulating factor information productivity (Selley, 1985). Minor spacing between rock grains is likely in spongy rock; these spaces will hold liquid, which can occasionally be water, oil, or gas. The permeability of the rock measures how easily this liquid may pass through it.

The precise estimation of permeability in complicated carbonate reservoirs is one of the most exciting aspects of well log analysis. Using well log data, numerous theories estimate permeability. Over time, many relationships have been developed to compute permeability based on known petrophysical properties or empirically derived relationships. Though, none of the existing well logging approaches can quantify it publicly. The Timur mode was employed to estimate formation permeability in the current investigation. Porosity is the most obvious determinant of permeability. This is because larger porosities indicate more and wider fluid flow channels. Different models may be used to predict permeability:

$$K = a * \frac{\emptyset^b}{Swir^c} \ldots\ldots\ldots\ldots\ldots\ldots\ldots\ldots (8)$$

The constants a, b and c for Timur, Morris-Biggs, and Schlumberger models are given below:

Morris-Biggs for gas: a= 6241; b = 6 and c = 2

Morris-Biggs for oil: a= 62500; b = 6 and c = 2

Timur: a = 8581; b = 4.4 and c = 2

Schlumberger: a = 10000; b = 4.5 and c = 2

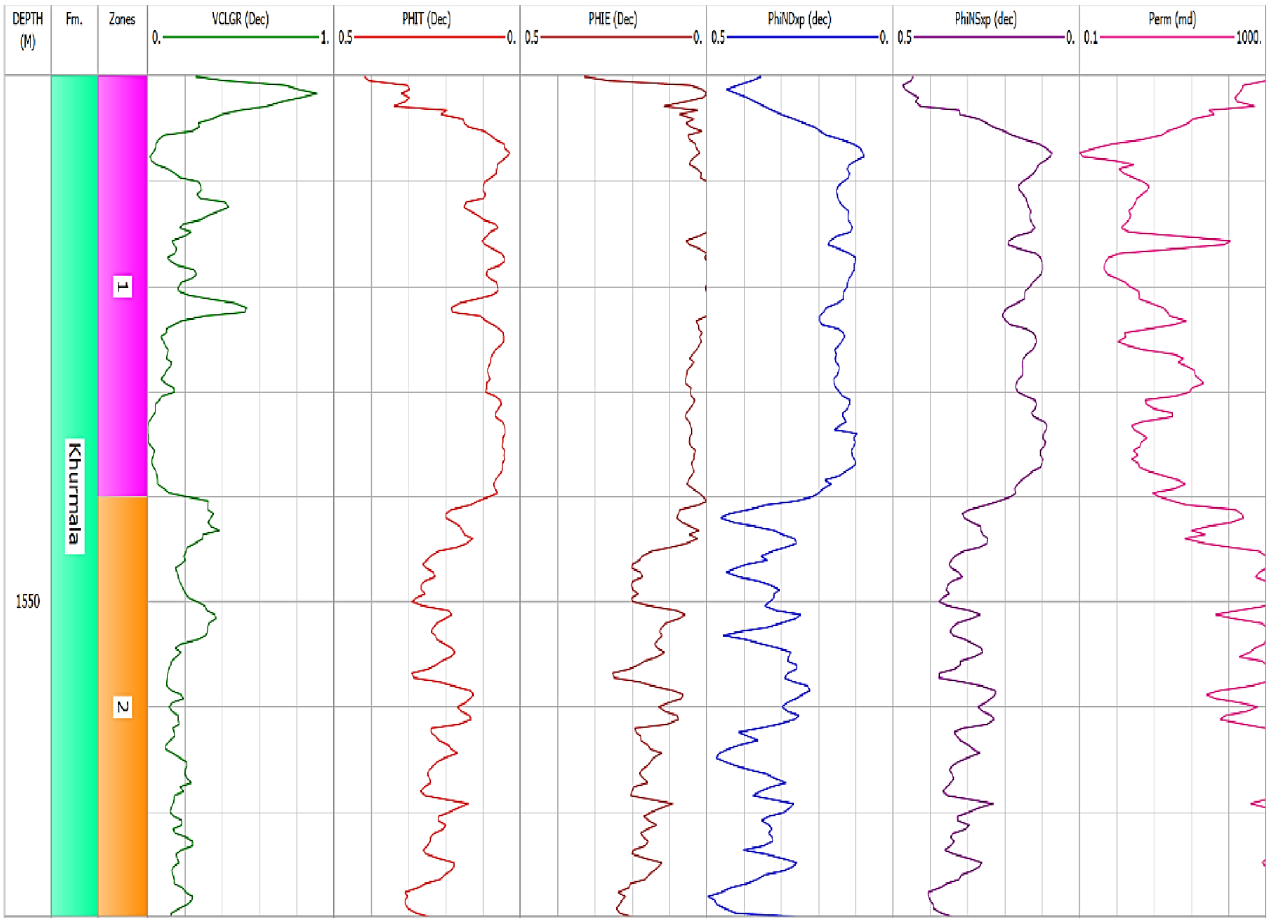

Abbreviations: Vcl GR: clay volume gamma ray; PHIT: Total porosity; PHIE: effective porosity; PhiND: neutron-density porosity; PhiNS: neutron-sonic porosity; Perm: Permeability.

Figure 13 Showing porosities, permeability and shale volume determination in the selected formation

4.6.2 Permeability Determination from outcrop

By flowing a fluid with a known viscosity through a predetermined sample with known dimensions at a predetermined rate and measuring the pressure drop across the core sample taken in outcrop section, or by setting the fluid to flow at a predetermined pressure difference and measuring the flow rate produced, permeability is measured on cores and samples taken from outcrop in the laboratory. We now need to draw a difference between the utilization of liquids and gaseous fluids. Liquids present a comparatively simple measuring problem since surface geological conditions nearly usually satisfy the requirements for laminar flow and incompressibility of the fluid. There are two issues with using gas as the fluid, which is a practice that is popular in the sector: Being a compressible fluid, gas will actually move more slowly when measured in volumes per second at the input (high pressure) end of the sample than at the outlet (low pressure), where it expands, even though it is moving through the core at the same mass per unit time. To account for the gas compression, the equation that was used to determine the permeability value from the observed values must be changed. Very few gas molecules may fill some of the smaller holes at low gas pressures. If this occurs, the rules we are applying fail, and their application results in an overestimation of permeability. Gas slippage or the Klinkenberg Effect is what causes this. As pressure is raised, the issue is less since there are more gas molecules per volume and the gas is compressed, and it doesn't exist with liquids because they are considerably denser than gases. By measuring the apparent permeability of the gas at various pressure differentials and creating a graph of the observed apparent permeability versus the mean pressure in the rock samples, gas slippage is adjusted for. The permeability is depicted as a function of $1/Pm = 2/(P_{in} + P_{out})$ if the input gas pressure is Pi and the output pressure is Po, as shown in Figure 4.7 Now, a straight line connecting the points should cross the y-axis at $1/Pm = 0$. This quantity, known as the

Klinkenberg permeability, really denotes the permeability at which a nearly perfect gas, under infinite pressure, transforms into a nearly perfect liquid. When measuring permeability using gas as the flowing fluid, Klinkenberg (1941) found that the findings were different from those obtained when measuring permeability with a liquid. When flowing gas is used to assess the permeability of a core sample, the result is always larger than when flowing liquid is used. This method is used for the outcrop samples that were obtained in the Khurmala Formation in Shaqlawa section, specifically the sample S3 & S11, where Klinkenberg discovered that for a given porous medium, as the mean pressure increased, the predicted permeability dropped. In contrast, in the other samples (S4 & S9) the permeability increase with increasing mean pressure (Pm)

.

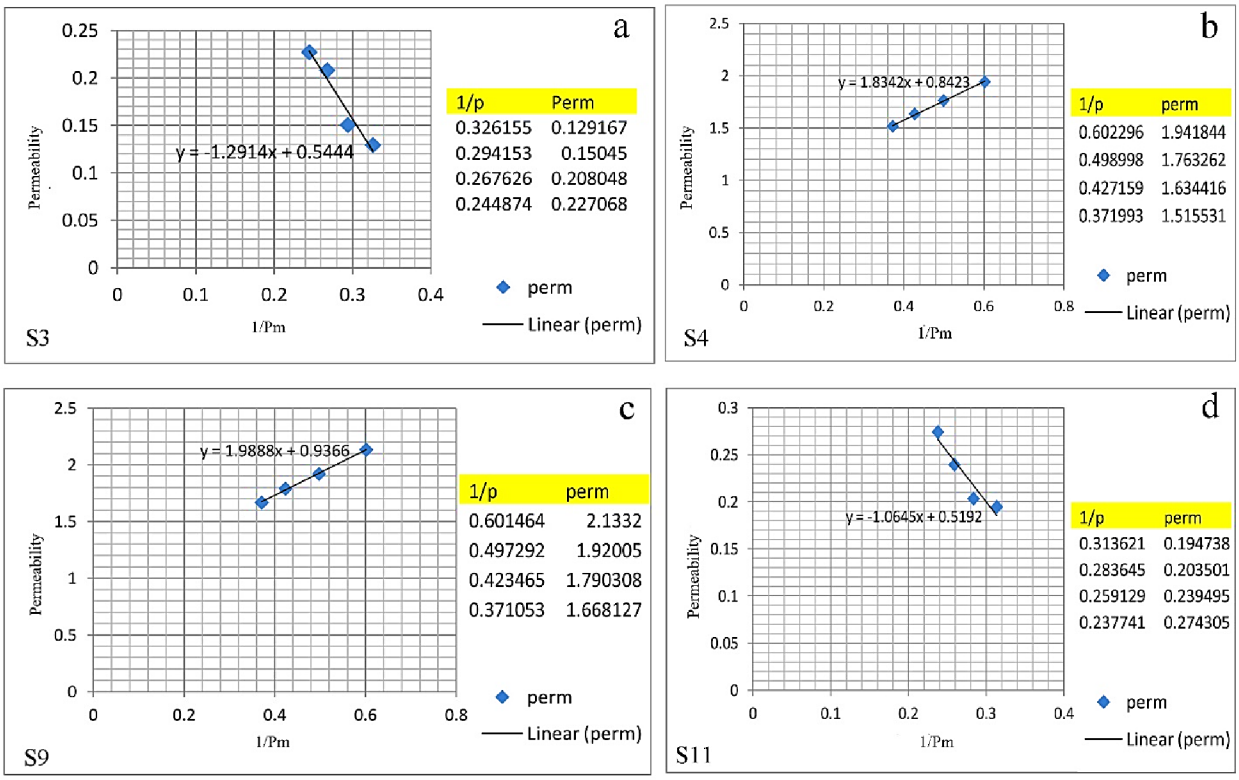

Figure 14 Relationship between Pressure mean and permeability for the analyzed samples in outcrop section

4.6.3 Relationship between porosity and permeability

Four core samples were taken in Shaqlawa area (outcrop section) to determine porosity and permeability of the Khurmala Formation. There are several ways to evaluate porosity. One is by thin sections, which offers apparent porosity, and another is through helium porosimeter study on core plugs, which yields effective porosity. (Fig 15) also depicts the link between porosity and permeability. The increase in porosity increases permeability because as the number of pores grows, so does interconnectivity, and as a result, permeability rises as well.

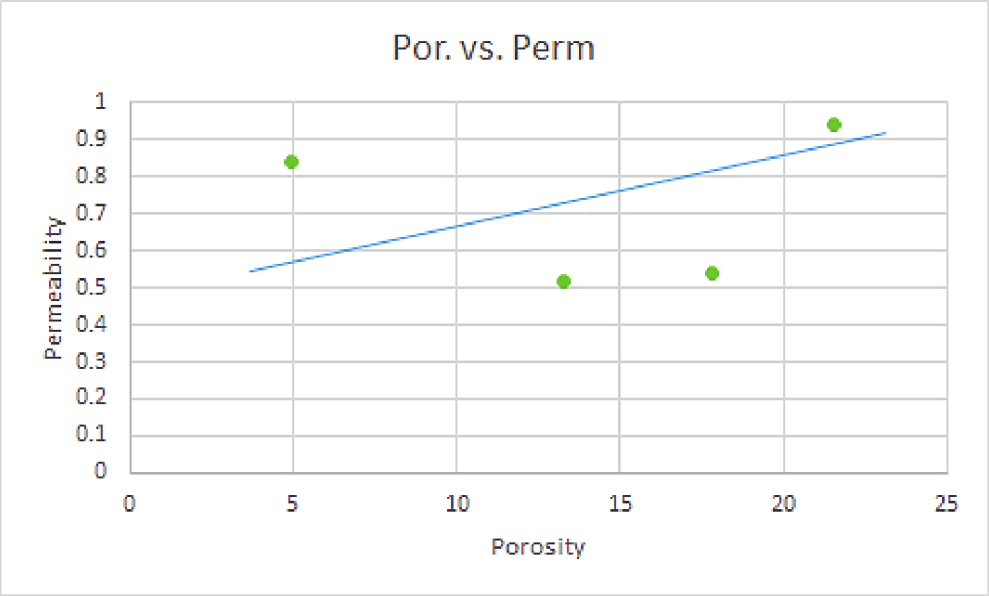

Figure 15 Relationship between porosity (%) and permeability (mD) for outcrop section

5.7. Thin section

The results for samples from Khurmala formation in Shaqlawa which known by thin section shown in (figs.15,16,17,18,19,20,21) :

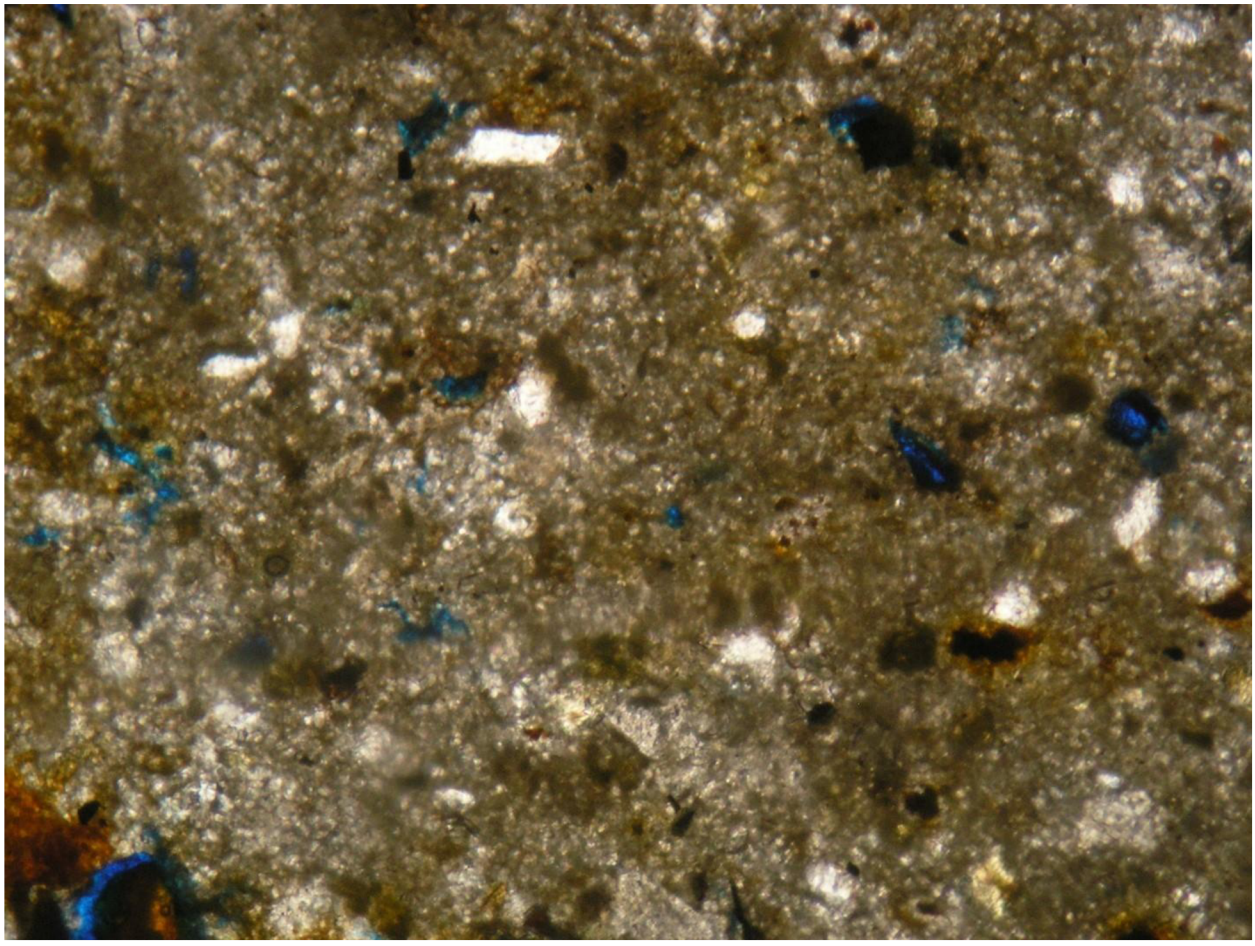

Figure 16 thin section sample for layer 2 in the Khurmala formation in Shaqlawa the porosity was 5 %

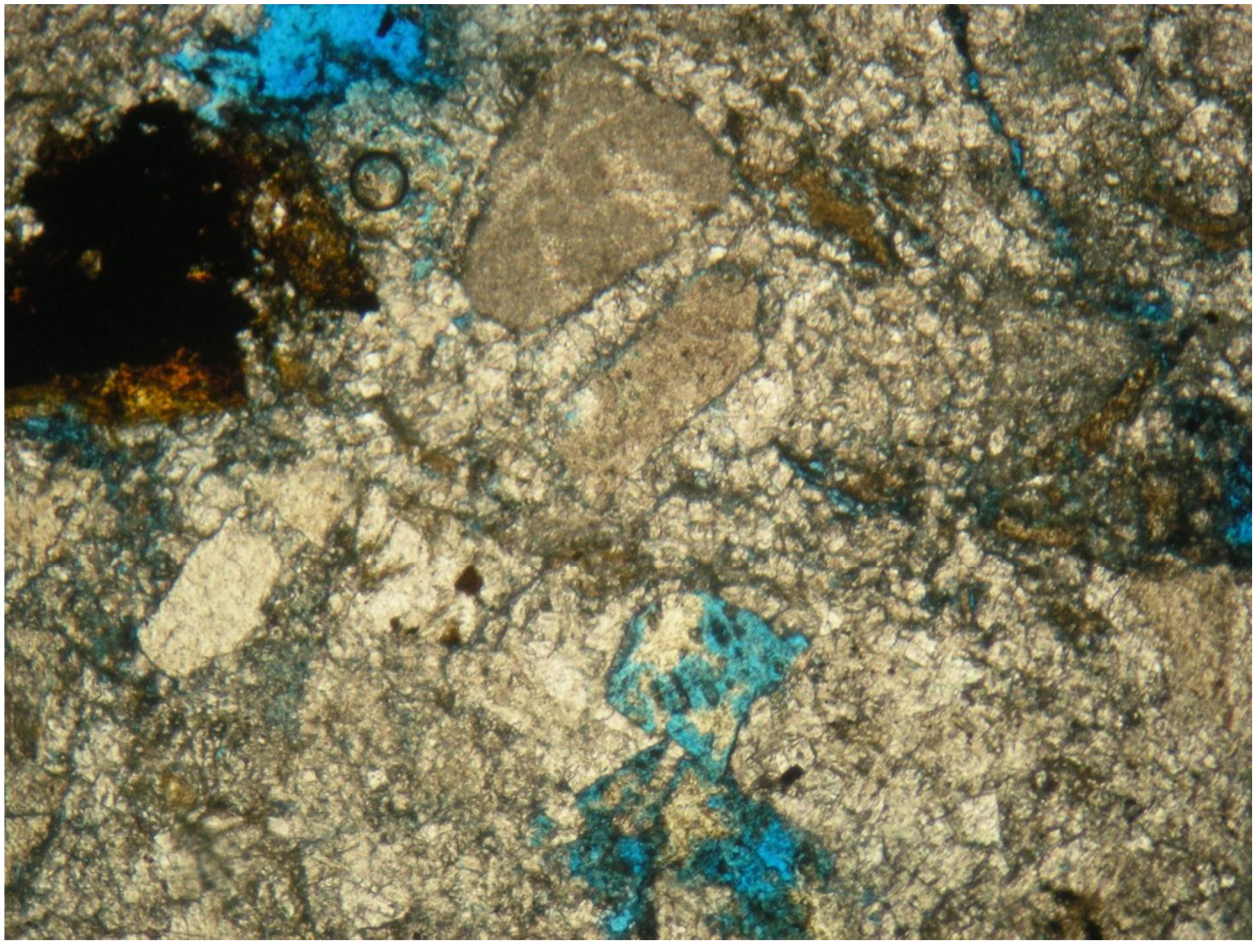

Figure 17 thin section sample for layer 7 in the khurmala formation in shaqlawa the porosity was 10 %

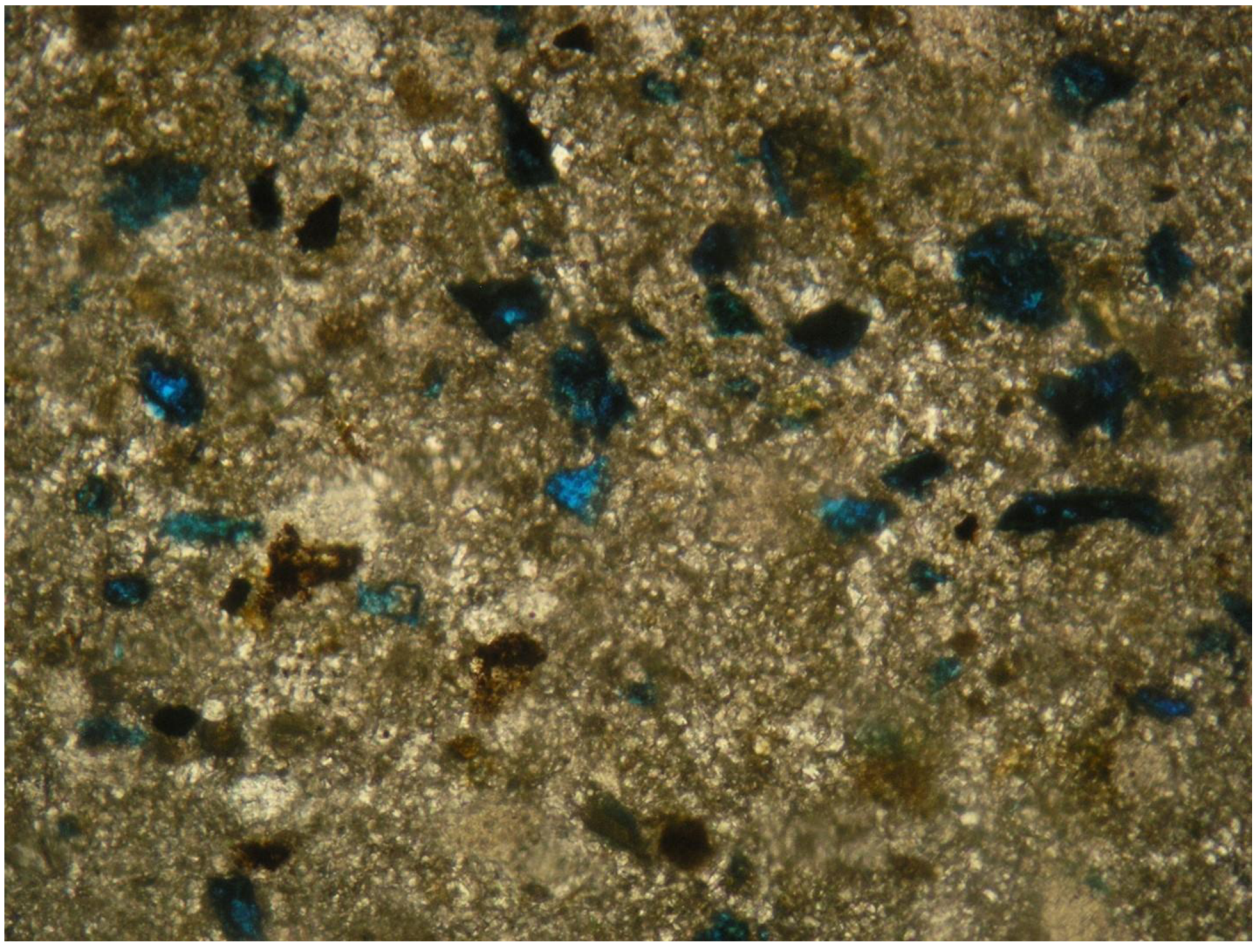

Figure 18 thin section sample for layer 7A in the khurmala formation in shaqlawa the porosity was 5 %

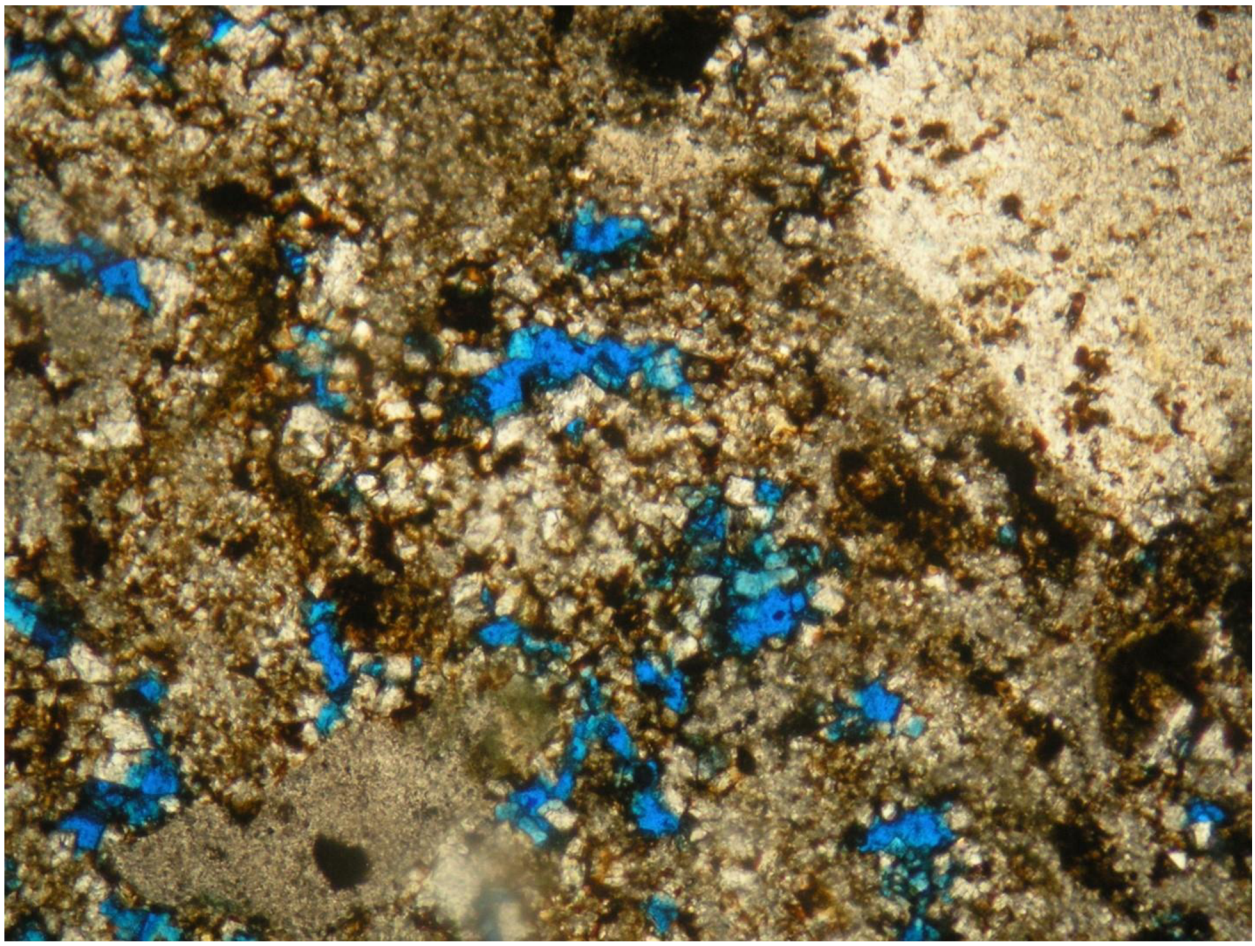

Figure 19 thin section sample for layer 7B in the khurmala formation in shaqlawa the porosity was 20 %

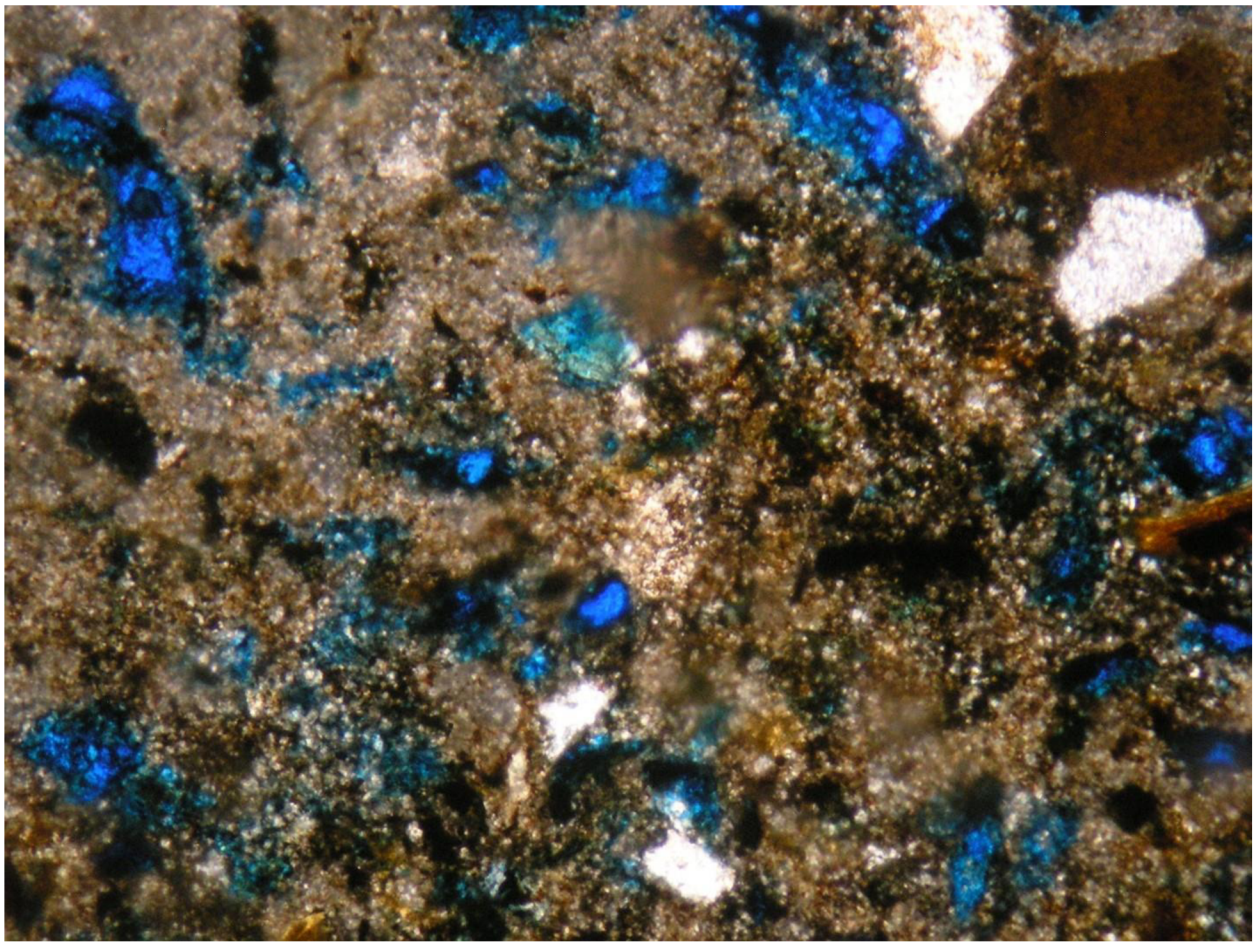

Figure 20 thin section sample for layer 5 in the khurmala formation in shaqlawa the porosity was 15 %

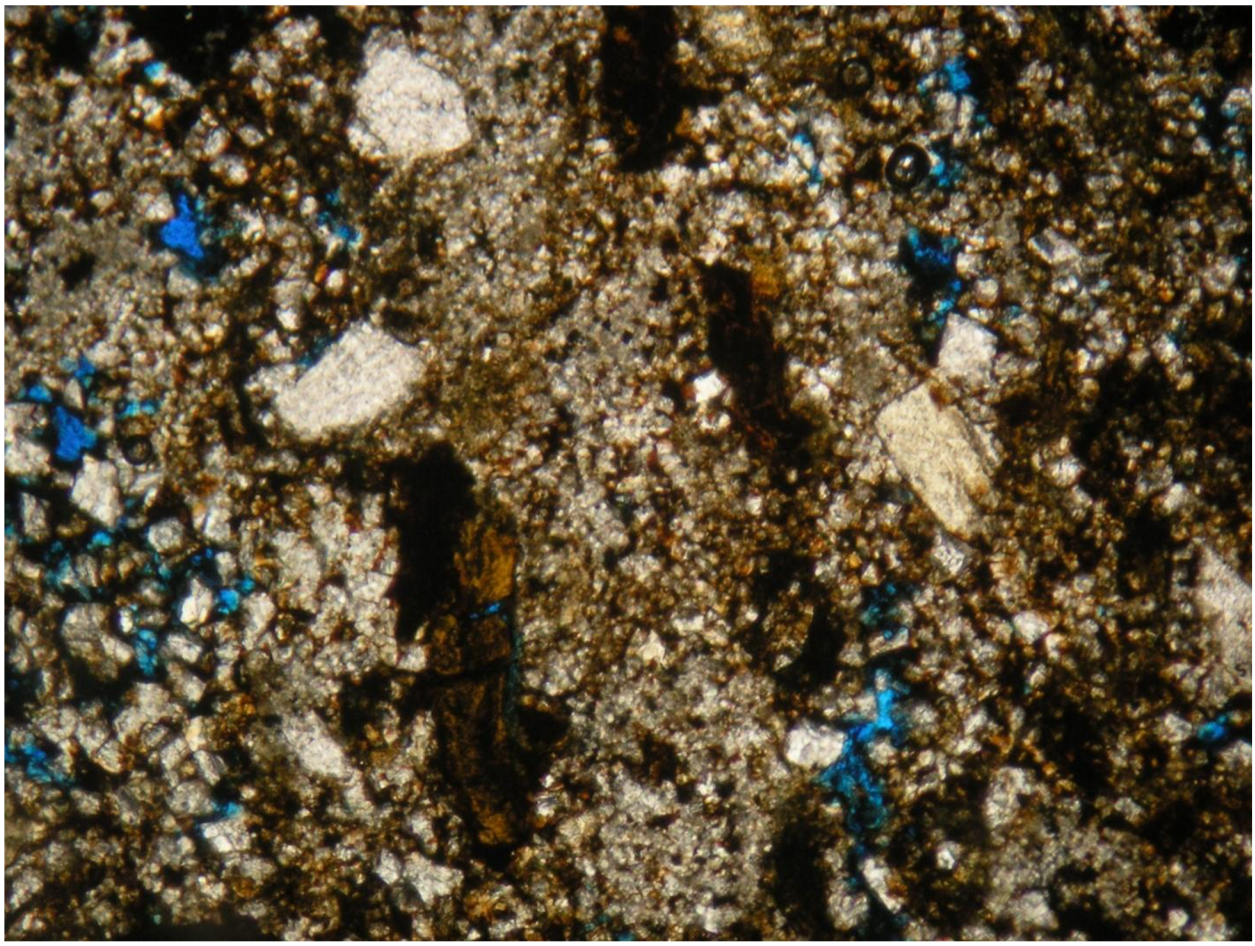

Figure 21 thin section sample for layer 8 in the khurmala formation in shaqlawa the porosity was 10 %

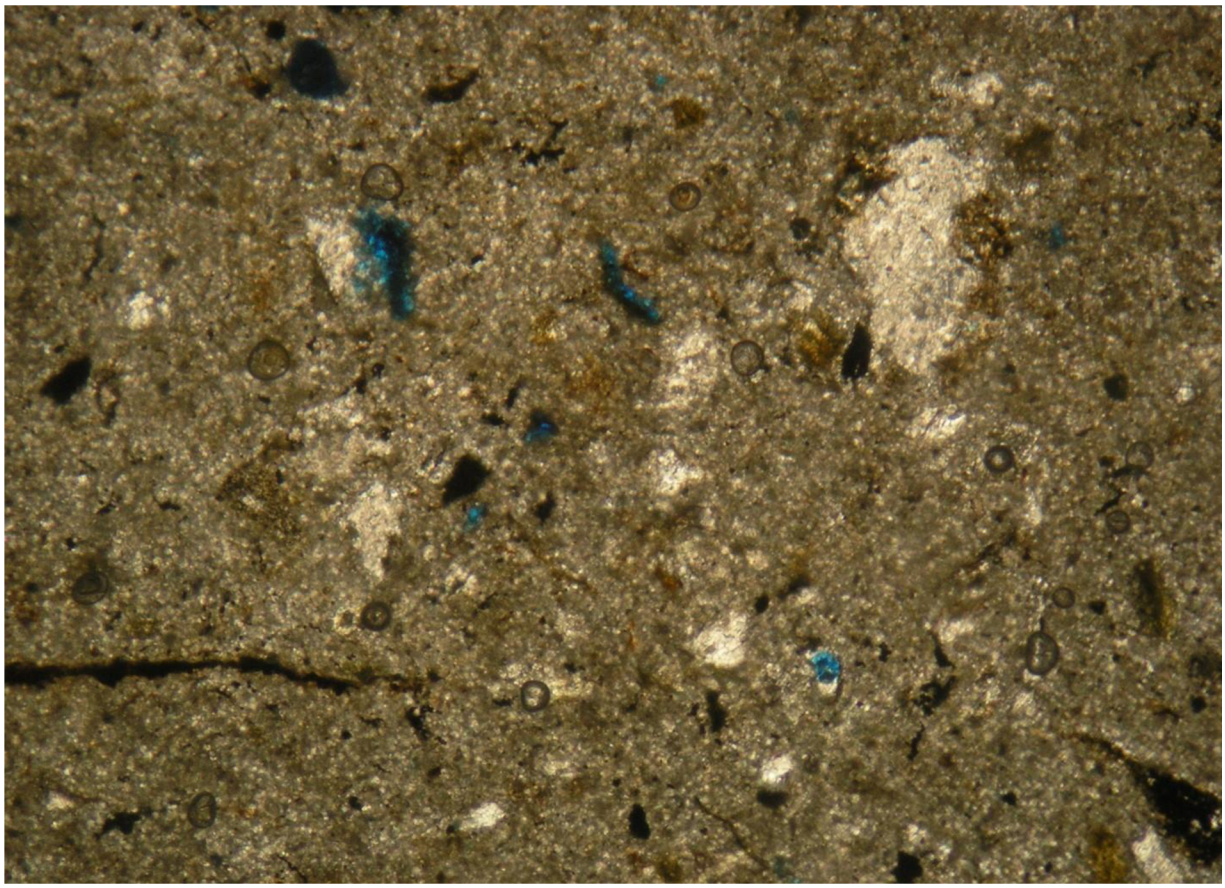

Figure 22 thin section sample for layer 16 in the khurmala formation in shaqlawa the porosity was 3 %

Chapter 5: Discussions

5. Pore pressure and fluid contact

5.1. Analysis of reservoir fluids

The volume of any given liquid in the pore space is known as its saturation, and the saturation is a percentage or fraction of the overall capacity to store fluids (porosity), which in essence holds any particular fluid. The determination of saturation and hydrocarbon movability reveals which permeable zones may be of interest (Pickett, 1966).

5.1.1 Water saturation (Sw)

It is the volume of pores that formation water has filled in a rock.

Decimal fractions or percentages are used to describe water saturation (Asquith and Krygowski 2004).

$$Sw = \left(\frac{a}{\emptyset^m} * \frac{Rw}{Rt}\right)^{\frac{1}{n}} \ldots\ldots\ldots\ldots\ldots\ldots \quad (9)$$

The Archie's (1942) formula is used to compute Sw of a reservoir's uninvaded zone:

$$Sxo = \left(\frac{a}{\emptyset^m} * \frac{Rmf}{Rxo}\right)^{\frac{1}{n}} \ldots \ldots \ldots \ldots \ldots \quad (10)$$

The moveable hydrocarbon can be identified by water saturation of the flushed zone (Sxo). If Sxo is larger than Sw, hydrocarbons in the flushed zone have most likely been transported or flushed out of the zone closest to the borehole by invading drilling fluids (Asquith, and Krygowski, 2004). The Sxo values in this study are more than Sw, indicating that the rocks under examination have a high moveable hydrocarbon content.

5.1.2 Water volume in bulk (Bvw)

Before the hydrocarbon migrated to the reservoir rocks and was recognized as connate water, the entire amount of bulk water that was preserved in sediments throughout deposition and lithification is referred to as bulk water volume (Tiab and Donaldson, 1996). The bulk volume of water (BVW) in the uninvaded zone is given by the product of the formation water saturation (Sw) and the effective porosity, while the bulk volume of water (BV_{SXO}) in the flushed zone is given by the product of the formation water saturation (Sxo) and the effective porosity (Spain, 1992).

The mobile hydrocarbon is represented by the area between BVWsxo and BVW, whereas the residual hydrocarbon is represented by the area between BVWsxo and φe

5.1.3 Saturation of hydrocarbons (Shc)

The following relationship may be used to infer the hydrocarbon saturation from the water saturation:

Hydrocarbon saturation is often classified as either non-exploitable or residual hydrocarbon (Shr) or exploitable or moveable hydrocarbon (Shm), as shown below:

$$Shc = 1 - Sw \quad \ldots\ldots\ldots\ldots\ldots (11)$$

$$Shc = Shr + Shm \quad \ldots\ldots\ldots\ldots\ldots (12)$$

On the computer processing interpretation (Fig. 23), mobile hydrocarbon can be observed in the lower part of the formation in subsurface section due to high porosity.

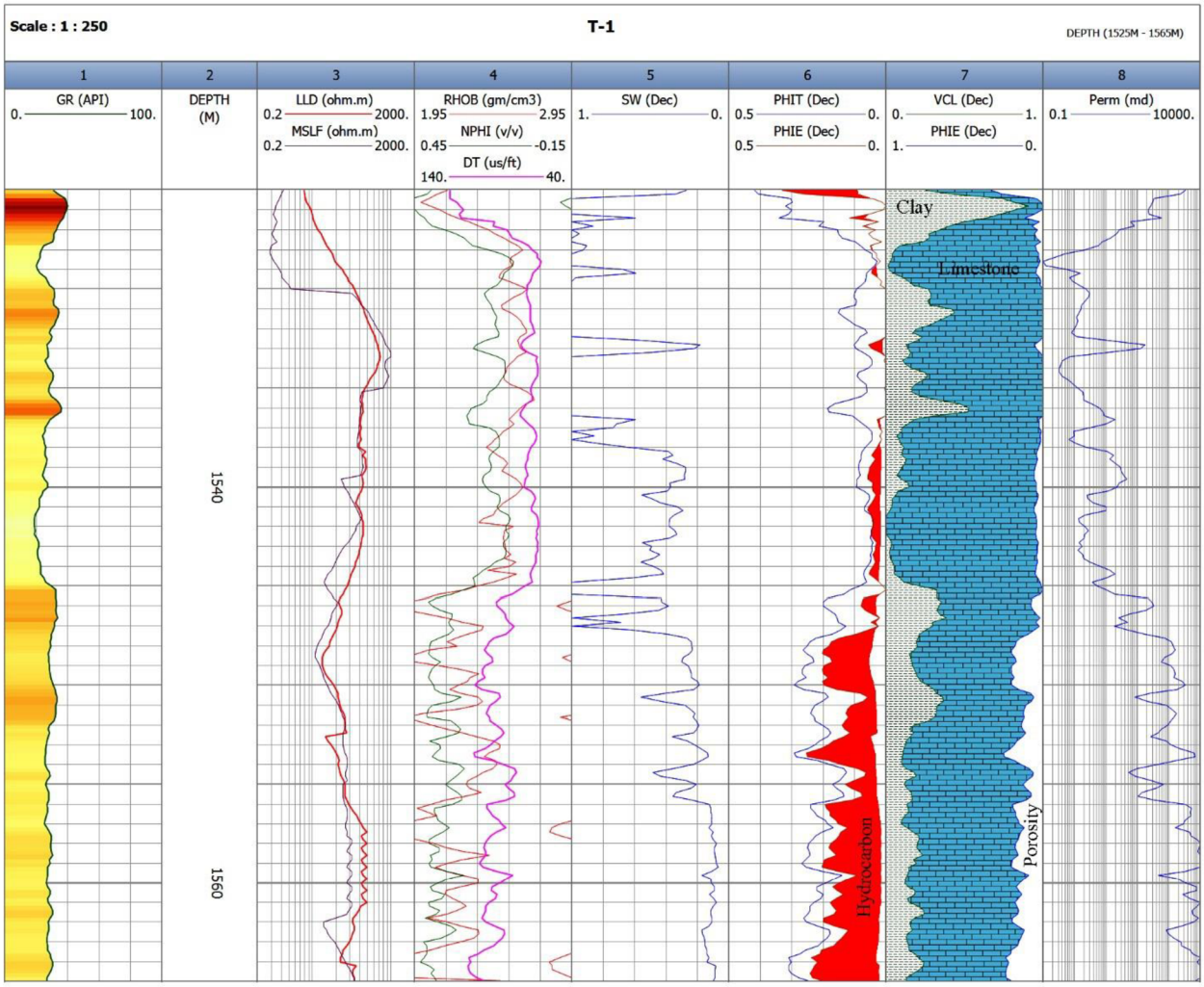

Figure 23 Computer processing interpretation (CPI) for the Khurmala Formation in Tawke oilfield, saturation and net pay have been shown in depth interval 1540-1565m

5.2 Pore pressure

Pore pressure sometimes referred to as formation pressure, is the force exerted by the fluid inside a formation's pores. Overpressure occurs when the pore pressure is greater than the hydrostatic pressure. For safe well design, effective reservoir modeling, and cost-effective drilling, knowledge of this pressure is crucial. The major goal of this work is to use well log data from one of the oil fields in the north of Iraq to estimate the formation pore pressure as a trustworthy mud weight pressure.

It can be classified as normal or abnormal depending on the size of the pore pressure. Normal pore pressure is the state in which the pore pressure equals the hydrostatic pressure. The permeable sediments link formations under normal pressure to a free surface. Pore pressure that is abnormally high (overpressure) or low (underpressure) compared to hydrostatic pressure is addressed (Swarbrick et al., 1998).

5.2.1 Pore pressure estimation methods

Various approaches to pore pressure estimation have been put forth. The first investigation into pore pressure estimation using shale parameters derived from well log data was done by Hottman and Johnson in 1965. This method was used to interpret any departure from the typical trend line in the observed parameters as an indication of anomalous pore pressure. Later, other researchers have successfully predicted pore pressure using well log data like as resistivity, sonic transit time, porosity, and others. The majority of these investigations are predicated on the concept that any changes in a region with normal pore pressure cause changes in petrophysical parameters such as compaction, porosity, and fluid motion.

As a result, any observable characteristics that may reveal these changes in some way can be employed in the interpretation and quantitative evaluation of pore pressure (Azadpour et al., 2015). Pore pressure estimation methods like as Eaton's, Bowers', and Holbrook's are widely utilized in the oil business.

Pore pressure is frequently calculated using Terzaghi's relationship and well log analysis. Based on this relationship, the overburden load is influenced by vertical effective stress and pore pressure. Terzaghi (1943) hypothesized the following relationship:

$$S = P + \sigma \ldots\ldots\ldots\ldots\ldots (13)$$

Where, *S* is the overburden pressure (the combined weights of formation solid and fluid); σ is the vertical effective stress (the grain-to-grain contact stress) and *P* represents the pore pressure.

One of the traditional techniques for predicting pore pressure is Eaton's approach, which views compaction disequilibrium as the primary process for overpressure development. Using well log data, Eaton (1975) established an empirical equation to calculate the pore pressure. This approach makes the assumption that, as Terzaghi's equation illustrates, pore pressure and vertical effective stress sustain overburden pressure. Eaton provided the empirical equation shown below for pore pressure prediction using sonic transit time in accordance with above (Equi 14):

$$Gp = Go - (Go - Gn)\left(\frac{\Delta tn}{\Delta to}\right)^{x} \ldots\ldots\ldots\ldots\ldots (14)$$

where, *Gp*, *Go*, and *Gn* are the pore pressure gradient, the overburden pressure gradient, and the hydrostatic pressure gradient respectively; *Δto* stands for the measured sonic transit time by well logging and *Δtn* is the normal sonic transit time in shale obtained from normal trend line; *x* represents the exponent constant.

Bowers' approach is based on effective stress to determine pore pressure. The essential step in this approach is to compute effective stress from velocity and then apply Terzaghi's equation to determine pore pressure. The major processes of overpressure creation in this approach are compaction disequilibrium and unloading owing to fluid expansion. Bowers (1995) suggested the following experimentally proven method for calculating effective stress under compaction disequilibrium conditions:

$$V = Vo + A\,\sigma^{B} \ldots\ldots\ldots\ldots\ldots\ldots (15)$$

where, *V* is the velocity at a given depth and *V0* stands for the surface velocity (normally 1500 m/sec); σ represents the vertical effective stress; *A* and *B* are the parameters obtained from calibrating regional

A pore pressure estimate technique for naturally fractured reservoirs was also put out by Holbrook (1999). Holbrook's approach does not need the establishment of any trend lines because it is based on the correlation between effective stress, mineralogy, and porosity in granular sedimentary rocks. In the North Sea, Holbrook was able to accurately forecast pore pressure in intervals of limestone, shaly limestone, and sandstone (Holbrook, 1999). The following equation is used in Holbrook's approach to determine the rock's effective stress:

$$\sigma = \sigma\, max\ x\ (1-\varphi)^{B} \ldots\ldots\ldots\ldots\ldots \quad (16)$$

where, σ_{max} is the maximum effective stress required to reduce the mineral porosity to zero and $\emptyset$ is porosity from well logs; β stands for the compaction strain-hardening coefficient for the type of minerals.

Weakley's approach

Because of the geological complexity of carbonate settings, determining pore pressure from log characteristics has always been difficult. As opposed to shales, they do not compress evenly with depth. Indeed, applying conventional pore pressure prediction methods to carbonate rocks does not necessarily result in an accurate forecast. Weakley (1990) devised a method for measuring formation pore pressures in carbonate settings by using sonic velocity patterns.

He used the sonic wave velocity trends for each portion of the formation while still using Eaton's theory. These formation portions were identified as the lithology changing index from well log replies. A smooth continuous sonic velocity log was created by joining the final value of the interval velocity trend from the previous lithology section with the first value in the next, which was then used to estimate the pore pressure using Eaton's approach. The detection of normal compaction trend line, normal compaction trend (NCT), and proper exponent constant x, which was initially 3 in Eaton's study and needs adjustment to be used in tight unconventional reservoirs, are the most effective parameters in Eaton's approach (Contreras et al., 2011).

The typically well log data must be used to calculate the normal compaction trend line. The abnormal pressure is shown by any departure from the usual trend line. Eaton's equation is expressed in terms of the exponent constant, x, to provide by

$$X = \frac{Log\ (\frac{Go-Gp}{Go-Gn})}{\log(\frac{\Delta Tn}{\Delta To})} \quad \ldots\ldots\ldots\ldots\ldots\ldots(17)$$

The gradient of normal hydrostatic pressure (Gn), according to studies conducted in the Middle East, is 10.5 kpa/m (Atashbari et al., 2015).

The studied oil field is located in the north Iraq. The reservoir formation is composed of shale, dolomite, and limestone. The studied formation includes Khurmala. it is a hard limestone formation of Paleocene-Eocene, The porosity in the upper part is relatively weaker than lower part of the formation.

Data from one well, including different petrophysical logs such as sonic transient time, gamma-ray, and density logs along with mud weight pressure data are used in this study to determine pore pressure. When there is evident noise, such as hole washouts or cycle skips on the sonic log, bad data is repaired. Additionally, software corrects environmental impacts such wellbore caving, mud salinity, mud pressure, and mud cake. This study's objective is to assess pore pressure in carbonate reservoirs using Weakley's methodology and compare the findings to pore pressure predictions made using the standard Eaton's method.

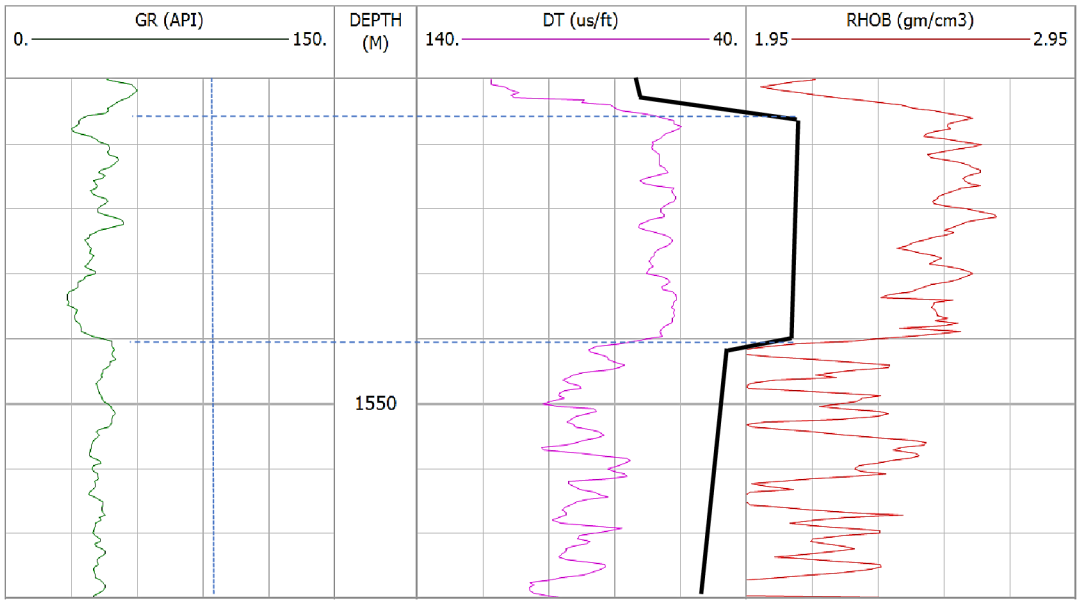

Figure 24 Lithology separations based on changes in petrophysical properties (GR, DT, and RHOB); trend lines are detected based on gamma ray peaks trend to the right for each lithology section.

Finding the lithology tops is the first stage in Weakley's method. Gamma ray, density, and sound logs are used to separate various lithologies in this process. Lithology tops are selected at the locations where the overall trend in the gamma-ray, density, or sonic logs changes.

The gamma ray peaks within lithological sections were examined, and the results revealed a tendency toward the right in the shale direction. It is possible to identify the sonic velocities, which correlate to the gamma ray peaks.

As seen in (Fig 24), trend lines have been created in relation to these sonic velocity peaks. According to Weakley's method, sonic trend lines are shifted at lithology transitions by merging the final interval velocity value from one lithological section with the first value from the next.

As shown in (Fig25) (a & b), this recalibrates the outcomes in a continuous relative interval sonic transient time (DT):

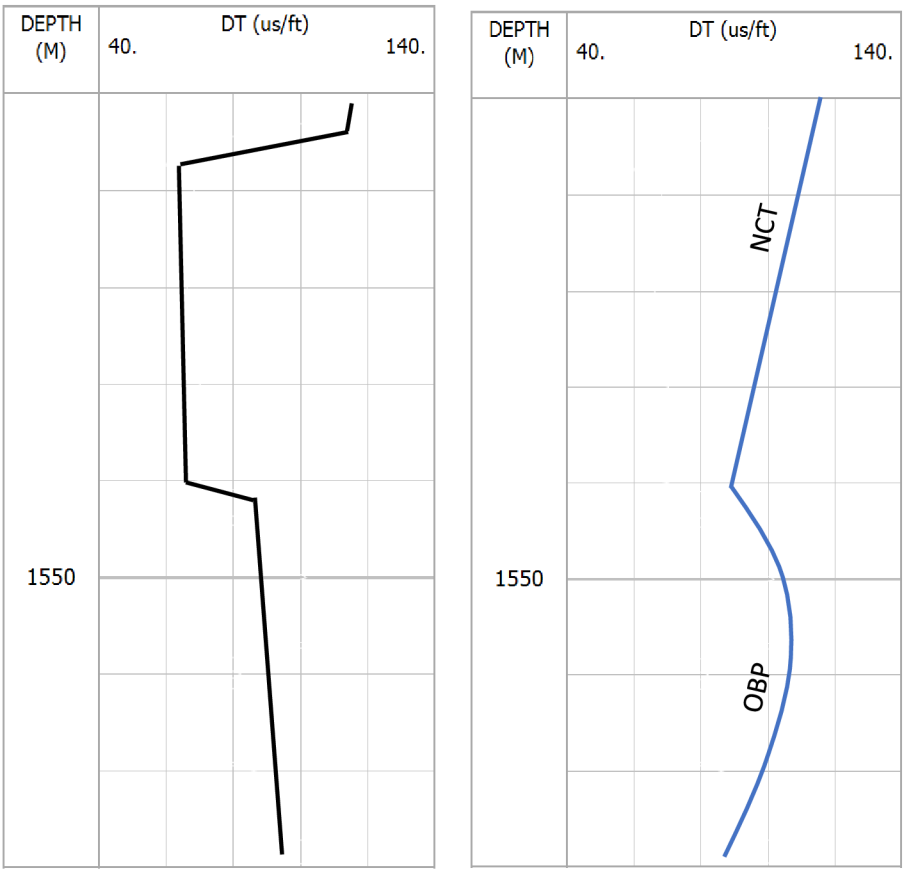

Figure 25 (a&b) (Sonic transient time calibration with Weakley's approach trend lines within lithologies a and b) DT log and recalibrated DT trend lines.

As shown in the (fig.26) the selected interval has no change in normal compaction trend while the other pressures have been changed, overburden pressure which represented by blue color depends on the total compressibility of the rock and is almost constant in the formation, Despite the fact that the measured hydrostatic pressure has been constant for a predetermined amount of time, the major cause of this rise (after depth 1550m) is an increase in density or the entry of additional fluids; The fluids in the voids are the primary cause of the considerable increases and decreases in pore pressure, which is in addition to the formation pressure, which observes a variation in the special value as a consequence of the different types of rocks from one layer to the others.

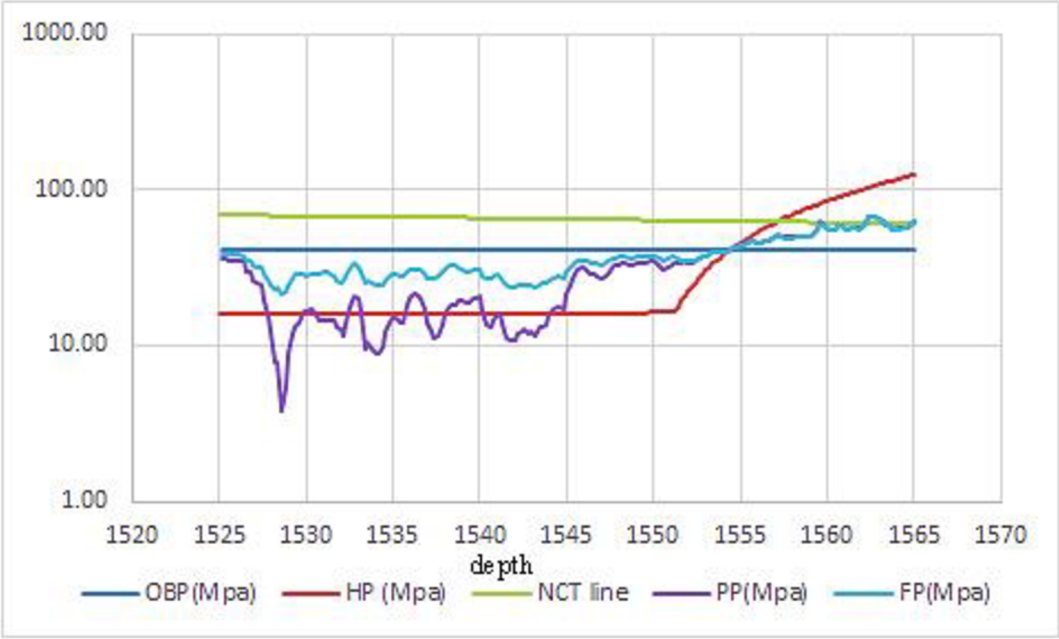

Figure 26 drawing depth vs. all parameters related to pressures (overburden (OBP), hydrostatic (HP), pore (PP)and formation pressure (FP) respectively)

Discussion the relation between porosity, water saturation, and pore pressure

The research region is located mostly in the Tawke oilfield and outcrop Shaqlawa district, between latitudes 36N and 44E. The Khurmala Formation is being studied by merging subsurface geology investigations, well log review, and petrophysical laboratory data in order to better understand the formation's hydrocarbon potentialities utilizing tawke-1 well.

Well logs of several forms for determining petrophysical parameters (shale content, porosity, and fluid saturation). The porosities were also calculated using the available acoustic, density, and neutron records. Based on the results of the flow line, background gases, mud density, and wireline logs, the outcomes were chosen for estimating the pore pressure for the Khurmala Formation. There found a correlation between pore pressure levels and hydrocarbon saturation.

The process of planning a well and evaluating a formation includes evaluating the formation pressures. For instance, knowing the pore pressure and fracture pressure is essential in order to optimize the mud density and provide adequate overbalance while drilling a well safely and inexpensively.

The Khurmala Formation in selected areas is composed of carbonate and shale, the characteristics of such reservoir are summarized as follows: the reservoir average parameter values were as value the shale content from 0.2%, effective porosity from 3 to 14%, while the water saturation from 20 to 28%, finally the hydrocarbon saturation average value 80%. The average of calculated formation pore pressure ranges from 0.4 ppg to 9 ppg. The studied well can be divided into two zones of pore pressure designated as normal pressure zone and abnormal pressure zone in this closed system reversal pressure has been developed due to the possibility of gas dissolved in water in the lower part, which has been a result of increasing pressure caused by sediment subsidence. Finally, the Khurmala Formation in the Tawke field is regarded as a promising reservoir with high pore pressure values and strong hydrocarbon potentialities.

Chapter 6: Conclusion

- The gamma ray log revealed that the volume of shale in the Khurmala Formation is 20%, though the shale volume increase toward the lower part of the Formation which has an impact on the reservoir properties of the rocks.
- The neutron-density cross-plot showed that the Khurmala reservoir consists mainly of limestone and dolomitic limestone, in addition to shale.
- Regarding to porosity model, fair and good porosity and permeability are present in the lower part of the Early Tertiary formation in this well and the porosity types are secondary porosity. The same result can be seen clearly in the outcrop section
- The saturation model shows that the upper part of the Khurmala Formation has no evidence of hydrocarbon but good movable hydrocarbons are present in the lower part of the formation.
- Pore pressure prediction and modeling based on sonic well-log provide results in the studied carbonate formation and claimed that the formation pore pressure occur after depth 1550m.
- Normal compaction trend has increase toward the more depth in the formation, whereas the all-other calculated pressure have been fluctuated due to changing in rock density and fluid inclusion from layer to another.

References

Adam, A., Swennen, R., Abdulghania, W., Abdlmutalib, A., Hariria, M. and Abdulraheem, A., 2018. Reservoir heterogeneity and quality of Khuff carbonates in outcrops of central Saudi Arabia. Marine and Petroleum Geology, 89, pp.721-751.

Alavi M 1994. Tectonics of the Zagros orogenic belt of Iran: new data and interpretations. Tectonophysics 229:211–238.

Alavi M 2004. Regional stratigraphy of the Zagros fold-thrust belt of Iran and its proforeland evolution. Am J Sci 304:1–20.

Al-Banna N. Y. Al-Mutwali M. M. Al-Ghrear J. S. 2006. Facies Analysis and Depositional Environment of Khurmala Formation in Bekhair Anticline –Dohuk Area, North Iraq, Iraqi Jour. Earth Sci., Vol.6, No.2, pp.13-22,

Al-Lihaibi S. F. 2012 Diagenesis of Khurmala Formation in Dokan Area, North Eastern Iraq, Iraqi National Journal of Earth Science, 2012, Volume 12, Issue 3, Pages 17-34

Al-Qayim B. Barzani A. T. 2021 Facies and stratigraphic associations of Sinjar and Khurmala Formation, Dohuk Area, Kurdistan Region, Iraq, Geography, Environmental Science, Geology

Al-Qayim, B.A. and Othman, D.H., 2010. Lithofacies association, dolomitization, and potentiality of the pila spi formation, taq taq oil field, Kurdistan region, NE Iraq. Iraqi Bulletin of Geology and Mining, 6(2), pp.95-114.

Al-Qayim, B. and Rashid, F., 2012. Reservoir characteristics of the albian upper qamchuqa formation carbonates, taq taq oilfield, Kurdistan, Iraq. Journal of Petroleum Geology, 35, pp.317-341.

AQRAWI, A.A.M., GOFF, J.C., HORBURY, A.D. and SADOONI, F.N., 2010. The

Petroleum Geology of Iraq: Scientific Press.

Asaad, I. S., Balaky, S.M., 2018. Microfacies analysis and depositional environment of Khurmala Formation (Paleocene-Lower Eocene), in the Zenta Village, Aqra District, Kurdistan Region, Iraq. Iraqi Bulletin of Geology and Mining, 14(2), 1-15.

Asaad I. Sh., Al-Haj M. A. and Malak Z.A. 2022 Depositional Setting of Khurmala Formation (Paleocene-Early Eocene) in Nerwa section, Berat Anticline, Kurdistan Region, Northern Iraq, Iraqi Geological Journal 2022, 55 (1F), 20-39

ASQUITH, G.B. and GIBSON, C. 1982. Basic well log analysis. Second edition AAPG, Tulsa, Oklahoma.

ASQUITH, G. and KRYGOWSKI, D. 2004. "Basic Well Log Analysis". Second edition.

Atashbari, V. and Tingay, M., Pore Pressure Prediction in Carbonate Reservoirs, in SPE Latin America and Caribbean Petroleum Engineering Conference, 2012.

Azadpour, M., Shad Manaman, N., Kadkhodaie-Ilkhchi, A., and Sedghipour, M.R., Pore Pressure Prediction and Modeling using Well-logging Data in One of the Gas Fields in South of Iran, Journal of Petroleum Science and Engineering, Vol. 128, p. 15-23, 2015.

BELLEN, R.C., DUNNINGTON, H.V., WETZEL, R. and MORTON, D. (1959)

Lexique Stratigraphic International. Asie, Fasc. 10a, Iraq, Paris p 333.

Bhuyan, K. and Passey, Q.R., 1994. Clay Estimation from Gamma Ray and Neutron-density Porosity Logs. SPWLA, 35thAnnual Logging Symposium, Tulsa.

Bowers, G., Pore Pressure Estimation from Velocity Data: Accounting for Overpressure Mechanisms Besides Undercompaction, SPE Drilling & Completion, Vol. 10, No. 2, p.89-95, 1995.

Contreras, OM, Tutuncu, AN., Aguilera, RM., and Hareland, GM., a Case Study for Pore Pressure Prediction in an Abnormally Sub-pressured Western Canada Sedimentary Basin, in 45th US Rock Mechanics/Geomechanics Symposium, 2011.

Doski J. 2019 Tectonic interpretation of the Raniya earthquake, Kurdistan, northern Iraq, J Seismol 23:303–318.

Eaton, B., the Equation for Geopressure Prediction from Well Logs, in Fall Meeting of the Society of Petroleum Engineers of AIME, 1975.

Fouad SFA (2014) Western Zagros fold–thrust belt, part II: the high folded zone. Iraq Bull Geol Mini Special Issue 6:53–71.

Ghafur, A.A. and Hasan, D.A., 2017. Petrophysical properties of the upper qamchuqa carbonate reservoir through well log evaluation in the Khabbaz oilfield. Journal of Science and Engineering, 1(1), pp.72-88.

Holbrook, P., A Simple Closed Form Force Balanced Solution for Pore Pressure, Overburden and the Principle Stresses, Earth Marine and Petroleum Geology, Vol. 16, p.303-319, 1999.

Hollis, C., 2011. Diagenetic on controls reservoir properties of carbonate successions within the Albian turonian of the Arabian plate. Petroleum Geoscience, 17, pp.223-241.

Hollis, C., Lawrence, D.A., Perière, M.D., Al Darmaki, F., 2017. Controls on porosity preservation within a Jurassic oolitic reservoir complex, UAE. Marine and Petroleum Geology, 88, pp.888-906.

Hottmann, CE. and Johnson, RK., Estimation of Formation Pressures from Log-derived Shale Properties, Journal of Petroleum Technology, Vol. 17, No. 06, p.717-722, 1965.

Hussein, D., Lawrence, J., Rashid, F., Glover, P. and Lorinczi, P., 2018. Developing Pore Size Distribution Models in Heterogeneous Carbonates Using Especially Nuclear Magnetic Resonance. In: Engineering in Chalk: Proceedings of the Chalk 2018 Conference. ICE Publishing, London. pp.529-534.

Jafarian, A., Fallah-Bagtash, R., Mattern, F. and Heubeck, C., 2017. Reservoir quality along a homoclinal carbonate ramp deposit: The permian upper Dalan formation, South pars field, Persian Gulf Basin. Marine and Petroleum Geology, 88, pp.587-604.

JASSIM, S.Z. and GOFF, J.C. 2006. Geology of Iraq. Czech Republic: Dolin,

Prague and Moravian Museum, Brno.

Krygowski, D.A., 2003. Guide to Petrophysical Interpretation. Wyoming University, Austin Texas USA. p.147.

Mukherjee S, Kumar N 2018. A first-order model for temperature rise for uniform and differential compression of sediments in basins. Int J Earth Sci 107:2999– 3004

Mzuri R. T and Omar A. 2016 Extraction and Analysis of Tectonic Lineaments using Geoinformatic Techniques, in Tawke Oil Field, Duhok area, Iraqi Kurdistan Region journal of zankoy slemani conference

Pickett, G.R. 1966. A Review of Current Technique for Determination of water saturation from logs. SPE 1446 p.

Rashid, F., Glover, P.W.J., Lorinczi, P., Hussein, D. and Lawrence, J., 2017. Microstructural controls on reservoir quality in tight oil carbonate reservoir rocks. Journal of Petroleum Science and Engineering, 156, pp.814-826.

Rashid, F., Hussein, D., Lawrence, J.A. and Khanaqa, P., 2020. Characterization and impact on reservoir quality of fractures in the cretaceous qamchuqa formation, Zagros folded belt. Marine and Petroleum Geology, 113, pp.104-117.

Rider, M.H. and Kenedy, M., 2011. The Geological Interpretation of Well Logs. Rider-French Consulting Ltd., Sutherland. p.280

Ryder Scott Company, 2011. Estimated Unrisked Discovered and Undiscovered Total Petroleum Initially in Place Attributable to Certaininterests in the Shaikan License Block, Kurdistan, Iraq. Report Prepared for Gulf Keystone Petroleum Ltd., Iraq.

Schlumberger 1974. Log interpretation, vol. II—applications. Schlumberger, New York

Schlumberger, 1997. Log Interpretation/Charts. Schlumberger Wireline and Testing, Houston, USA.

Schlumberger, 2012. Definition of porosity: How porosity is measured. Oil Field Review Autumn, 24(3), pp.63-64.

SELLEY, R.C. (1985-1998) Elements of petroleum geology. San Diego – London,

UK: second edition, Academic press.

Sherwani, G.H. and Zangana, H.A. 2017. Reservoir characterization of early jurassic formations in selected wells in the duhok governorate, Iraqi Kurdistan region. Journal of Science and Engineering, 1(1), pp.11-18.

SPAIN, D.R. 1992. Petrophysical Evaluation of a slope Fan / Basinfoor Fan

Complex, Cherry Canyon Formation. AAPG Bulletin. 76(6). p.805-827.

Swarbrick, B. E. and Osborne, M. J., Mechanisms that Generate Abnormal Pressures, an Overview, Memoirs-American Association of Petroleum Geologists, p. 13-34, 1998.

Terzaghi, K., Theoretical Soil Mechanics, 1943.

TIAB, D. and DONALDSON, E.C. (1996) Petrophysics, Theory and Practice of Measuring Reservoir Rock and Fluid Transport Properties. Huston, Texsas.

Weakley, R. R., Determination of Formation Pore Pressures in Carbonate Environments from Sonic Logs, in Annual Technical Meeting, Petroleum Society of Canada, 1990.

Wiley, R. and Pachett, J.G., 1990. CNL (Compensated Neutron Log) Neutron Porosity Modeling, a Step Forward. SPWLA 30th Annual Logging Symposium.

ZebariM(2013) Geometry and evolution of fold structures within the high folded zone: Zagros fold-thrust belt, Kurdistan region-Iraq. MSc Thesis, University of Nebraska-Lincoln, p.91